Trends on Carbon Nanotube-Based Flexible and Wearable Sensors via Electrochemical and Mechanical Stimuli: A Review

Anthony Palumbo, *Member, IEEE*, Zheqi Li, *Student Member, IEEE*, and Eui-Hyeok Yang, *Senior Member, IEEE*

***Abstract*—Flexible and wearable sensors increasingly draw attention owing to their advantages of providing lightweight, portable, wearable, or implantable capabilities. Along with the development of flexible materials toward wearable devices, flexible sensors operating via electrochemical and mechanical stimuli demonstrate promise to fulfill potential healthcare and robotics applications, including artificial muscles, health monitoring, human motion detection, soft robotic skin, and human–machine interfaces. This review focuses on carbon nanotube (CNT)-based flexible sensors to detect diverse chemical species and mechanical forces. Often, combined with polymers to imbue flexibility, CNT-based flexible sensors enable specific and stable detections of mechanical deformations and electrochemical analytes while withstanding various mechanical loads, including stretching, bending, and twisting.**

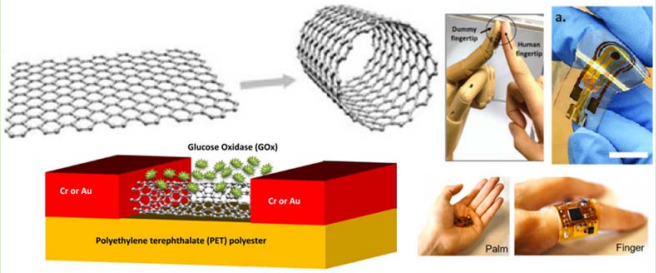

***Index Terms*—Carbon nanotubes (CNTs), electrochemical sensor, flexible sensor, mechanical sensor, wearable electronics.**

I. Introduction

ALONG with the development of flexible materials, flexible sensors have become increasingly promising to fulfill applications in healthcare and robotics [1]. Interests within industrial applications include artificial muscles [2], health monitoring [3], human motion detection [4], soft robotic skin [5], and human–machine interfaces [6]. Sensors typically composed of rigid materials, such as metals and inorganic semiconductors, often cannot undergo high-strain applications. Therefore, increasing demand for flexible sensors is present, and strategies and new materials are being researched to achieve high performance as flexible systems to withstand the strain toward wearable technologies [7].

Owing to their remarkably superior carrier mobility, stability, and outstanding mechanical flexibility, carbon nanotubes (CNTs) are promising nanomaterials for flexible or stretchable microelectronics [8]. As shown in Fig. 1, CNTs can be viewed as 1-D nanotubes of graphene, defined by a hexagonal arrangement of carbon atoms. A seamless cylindrical single-walled CNT (SWCNT) can be understood as a rolled graphene sheet in its geometry. They are characterized by the resulting structural parameters of diameter and chirality, defined by indices (n, m). Because of their versatility and use in various electronic applications, CNTs may be characterized by differing electrical characteristics depending on these indices (n, m) such that, when the difference of indices $(n-m)$ equals the multiples of 3, then the CNT is metallic, and for all the other values, it is semiconducting. Furthermore, the bandgap of a semiconducting nanotube can be tailored, as it is inversely proportional to its diameter. Materials with tailorable bandgaps are useful for sensitive semiconducting sensing capabilities, such as field-effect transistors (FETs) [9]. These properties enable us to use CNTs in diverse electronic applications, which require a specific design of an electrode surface interfaced with its surrounding environment to detect exclusive signals and convert them to meaningful and quantifiable information.

CNT-based sensors have drawn increasing attention toward sensing both electrochemical and mechanical stimuli for wearable applications [10], [11], [12]. Electrochemical sensors typically contain an analyte that binds to a receptor and a transducer (electrode) to convert the chemical reaction into an electrical signal [13]. Here, the electrode often oxidizes or reduces the analyte of interest, and the produced current is monitored to collect concentration data within the sample of interest. Owing to their high surface-to-volume ratio, CNTs

Manuscript received 19 July 2022; revised 11 August 2022; accepted 11 August 2022. The associate editor coordinating the review of this article and approving it for publication was Prof. Mahesh Kumar. *(Corresponding author: Eui-Hyeok Yang.)*

The authors are with the Mechanical Engineering Department, Stevens Institute of Technology, Hoboken, NJ 07030 USA (e-mail: ehyang@ieee.org).

Digital Object Identifier 10.1109/JSEN.2022.3198847

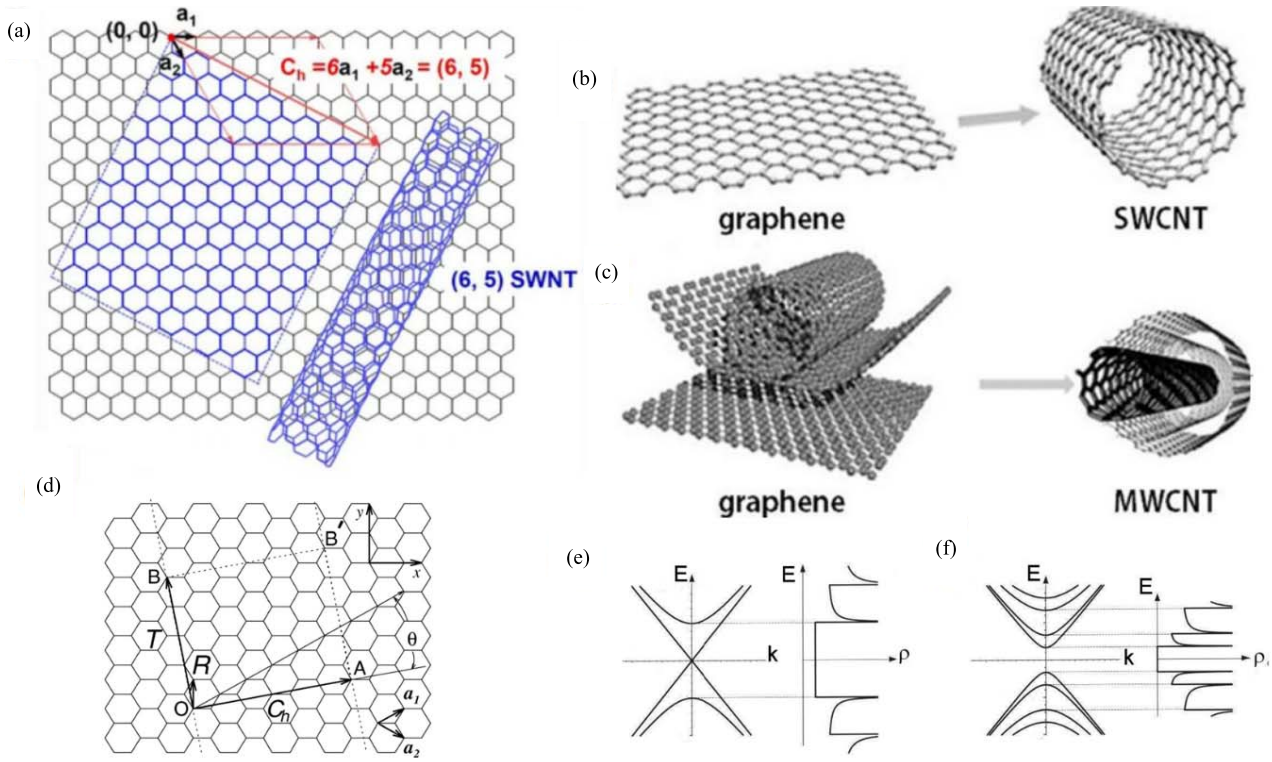

Fig. 1. (a) Schematic illustration of a (6, 5) SWNT rolled up from a graphene sheet. The chiral indices (n, m) uniquely define the structure of an SWNT [173]. Graphene and CNTs as (b) SWCNT and (c) MWCNT structures [174]. (d) Unrolled honeycomb lattice of a nanotube. A nanotube can be constructed when connecting sites O and A and sites B and B∗. OA and OB define the chiral vector and the translational vector T of the nanotube, respectively. The rectangle OAB∗B defines the unit cell for the nanotube. The figure is constructed for an (n, m) = (4, 2) nanotube [40]. (e) Schematic band structure and density of states of metallic nanotube: the crossing bands at the Fermi level result in a finite density of states and metallic behavior. The other noncrossing bands cause van Hove singularities. (f) Schematic band structure and density of states of semiconducting nanotube: there are no allowed states at the Fermi energy, and the tube behaves as a semiconductor. van Hove singularities appear at the band minima and maxima as a result of the 1-D electronic system [41]. Figures reprinted with permission from [173] Copyright 2019, Springer Nature. Figures reprinted with permission from [174] Copyright 2014, Frontiers. Figures reprinted with permission from [40] Copyright 2004, Annual Reviews. Figures reprinted with permission from [41] Copyright 2010, Bentham Science Publishers.

are promising as sensing materials. The tube structure of CNTs can be compared to graphene sheets rolled into tubes. Therefore, the electronic properties of CNTs are like the basal planes of pyrolytic graphite (BPPG). Furthermore, the end regions of CNTs have higher curve strain, so the opening ends can combine various oxygen-containing groups, possessing properties like the edge locations of BPPG [14]; this structure can help to accumulate more biomolecules, which leads to enhancement of the probe's sensitivity [15].

Detecting both mechanical and electrochemical stimuli with flexibility is critical to various fields that undergo mechanical deformation, such as flexible displays [16], wearable sensors [17], flexible electronic papers [18], and wound monitoring patches [19]. For example, flexible sensors can be used to monitor individuals' biometrics *in vivo* or on one's skin for active dynamic use, increasing self-monitoring capabilities in a growing telehealth industry [20], or provide sensory feedback to enable new capabilities in robotics [21]. In addition, flexible damage monitoring sensors are advantageous for the easy installation of devices on complex geometries, such as switch rails, providing data that can be employed to minimize risk and negative consequences [22], [23]. For these reasons, the development of CNT-based flexible sensors is a growing focus among the research and industry communities alike due to their potentially revolutionary applications [24].

As introduced, a greater focus on CNT-based flexible electronics has recently coincided with an increase in review papers related to this topic area. A review article was published about CNT-based flexible electronics for flexible circuits, displays, RF devices, and biochemical sensors [25]. This article reviews the progress of CNTs in flexible electronics by describing their mechanical and electrical properties. In 2019, another review was published on electrochemical hydrogen peroxide nanotube-based biosensors [26]. This article mainly focuses on CNT-based electrochemical hydrogen peroxide sensing strategies, which provides us with several design directions for flexible electrochemical sensors. Another review article on CNT-based flexible sensors focuses broadly on manufacturing strategies. More recently, a review was published focusing on CNT-based flexible mechanical sensors, giving the details for fabricating CNT-based flexible conductive networks for resistive-type strain sensors [27].

Here, we review the most recent advances in flexible and wearable sensors based on CNTs. First, we describe the structure and material properties of CNTs, followed by a discussion of synthesis strategies and immobilization techniques

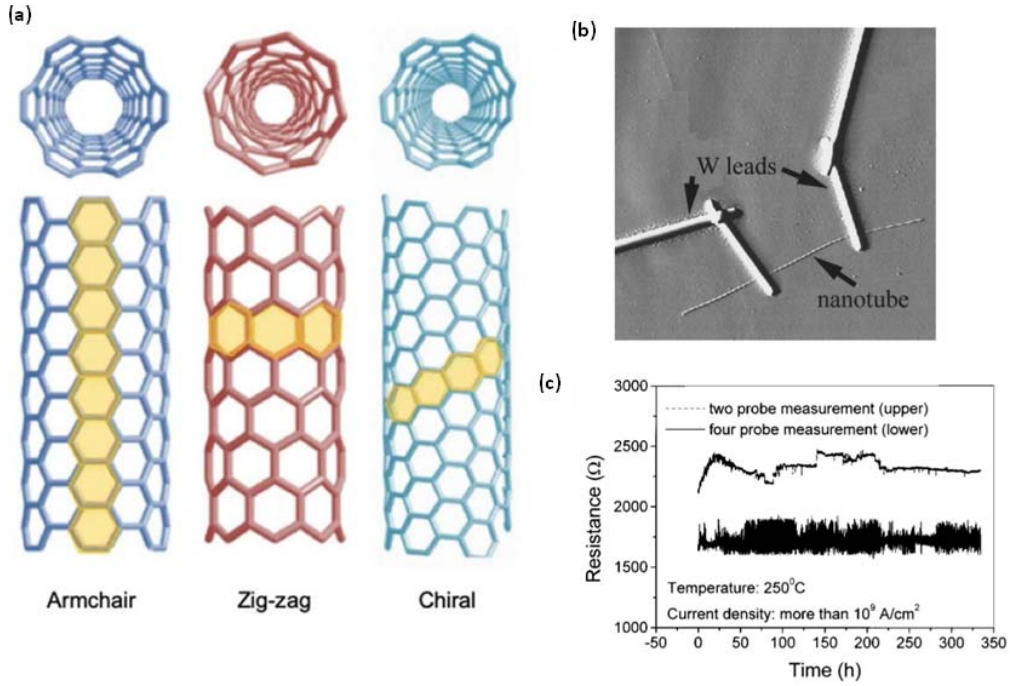

Fig. 2. (a) Schematic theoretical model for SWCNTs with chirality [102]. (b) AFM image of two tungsten leads connecting an individual CNT to measure. (c) Resistance stability of the CNT for two probe and four-probe measurements resulting in current densities higher than 109 A/cm^2 at ambient temperatures of 250 °C in the air [32]. Figures reprinted with permission from [102] Copyright 2020, Springer Nature. Figures reprinted with permission from [32] Copyright 2001, American Institute of Physics.

of CNTs on substrates, including elastomeric polymers and their combinations within sensor designs. Furthermore, we feature various applications of CNTs as flexible sensors via mechanical and electrochemical stimuli and durability toward wearable applications. Finally, we highlight the future trends and perspectives in developing flexible CNT-based sensors.

II. CNTs

A. CNT Overview

The unique mechanical and electrochemical properties of CNTs enable the flexibility and wearability of CNT-based sensors. Here, we start from the origin to introduce the structure and the properties of CNTs.

CNTs were discovered in 1991 and have been well studied and demonstrated in diverse applications in both industry and research [28]. A single CNT is a cylindrical rolled-up layer(s) of graphene with a chemical composition of carbon atoms arranged in a hexagonal pattern, as shown in Fig. 1(a). The carbon atoms in CNTs are chemically bonded by sp^2 bonds, and the resulting carbon–carbon covalent bonds are valued as some of the strongest bonds [29], [30].

CNTs are divided into either SWCNTs or multiwalled CNTs (MWCNTs). SWCNTs typically have diameters between 0.8 and 2 nm as a single rolled sheet, whereas MWCNTs are formed by concentric graphene layers that typically result in diameters between 5 and 20 nm. Geometric properties of CNTs can be controlled by adjusting the growth parameters, an example of which is the CNT length, which has been demonstrated to range from less than 100 nm to up to 0.5 m [31]. As shown in Fig. 2(a), the orientation of the carbon-bonded hexagonal lattice, referred to as chirality (i.e., armchair, zigzag, or chiral), results in SWCNTs [see Fig. 1(b)] that are either semiconducting or metallic. Armchair nanotubes have identical chiral indices and pertain to high conductivity. Alternatively, zigzag nanotubes are semiconducting with an orientation characterized by rotating the graphene sheet 30° from a chiral orientation. On the other hand, MWCNTs [see Fig. 1(c)] are usually highly conductive metallic materials, carrying currents up to 109 A·cm^{-2} [32]. Owing to their exceptionally high Young modulus, stiffness, flexibility [33], and unique geometry, CNTs have been used in numerous applications, including filtration [34], sensing [35], energy storage [36], electronics [37], catalyst supports [38], and electron field emitters [39].

A CNT is specified by the chiral vector, as shown in the equation: $C_h = na_1 + ma_2 = (n, m)$. From this equation, the chiral vector is represented by a pair of indices, n and m, which are two integers that correspond to the number of unit vectors along with the two directions in the honeycomb crystal lattice of graphene. When $m = 0$, the nanotube is called "zigzag"; when $n = m$, the nanotube is called "armchair"; all other configurations are designated chiral. Fig. 2 shows the three different types of SWCNTs: armchair, zigzag, and chiral. As shown in Fig. 1(d), there are two crystallographic equivalent sites, O and A, on a 2-D graphene sheet, and a chiral vector connects these two sites [40]. Here, the chiral vector makes an angle θ with a zigzag. For different angles θ, CNTs can be divided into armchair nanotubes, zigzag nanotubes, and chiral nanotubes. The diameters of CNTs can also be calculated by indices (n, m). The allowed k-points in the Brillouin

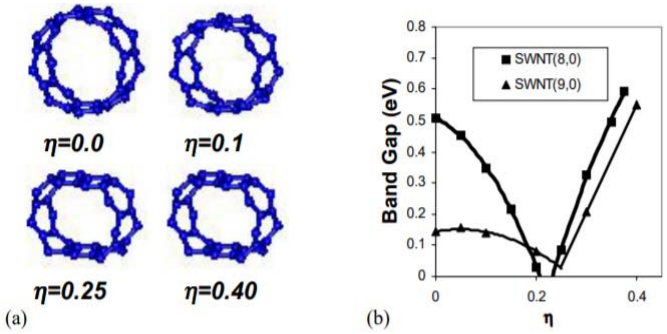

Fig. 3. (a) Flattening of (9, 0) CNT with four different degrees of deformation. (b) Energy band gap as a function of η for (8, 0) and (9, 0) SWNTs. The continuous lines are fit through either a quadratic or linear function [248].

zone are confined to parallel lines in the zone-folding approximation. The (n, m) pair of integers can determine the length and orientation of these lines and the coordinate of the K point. As shown in Fig. 1(e) and (f), whether any of the allowed K-lines crosses the K point can be used to measure the arrangement of carbon atoms, which can influence the electrical properties of CNT. K-lines crossing the K point means that there are allowed states at the Fermi level—the CNT exhibits metallic behavior. There are no K-lines that can cross K point means that there are no allowed states at the Fermi level; the CNT processes semiconducting behavior [41].

Depending on the unique electrical properties of CNTs, specific types of CNTs are often selected for the design of flexible sensors. For example, CNTs are good candidates for developing electrochemical sensors, where metallic CNTs enable their direct use as the working electrode for three-electrode electrochemical sensors. Moreover, metallic CNT-based electrodes allow fast electron transfer kinetics [244], helping electrochemical sensors achieve a fast response. On the other hand, the CNTs with semiconducting properties are key materials for developing FET-based electrochemical sensors for applications, including label-free DNA detection [245] and gas sensing [246]. In addition, the combination of p-type and n-type semiconducting materials has synergistic effects via various oxidative-reductive active sites during the electrochemical sensing process [247], facilitating the adsorption-diffusion of sensing targets on the CNTs' modified electrode.

For mechanical sensors, different chiral vectors of CNTs can provide various design directions. For example, the relationship between electrical properties and mechanical deformation was explored for CNTs: Mechanical deformation changes the chiral vectors of CNTs, realizing the transition between metallic and semiconducting. Fig. 3 shows the relationship between deformation parameter η and the band gap of CNTs. The deformation parameter η is defined as $\eta = (D_0 - d)/D_0$, where D_0 is the original diameter of the nanotube and d is the smallest diameter of the flattened cross section of the CNT [248]. Using this principle, the CNTs can be applied to measure the strain and deflection.

B. CNT Fabrication

Various methods can produce MWCNTs and SWCNTs with different scales. Here, we introduce three typical CNT synthesis methods and show the difference in growth conditions. Three primary techniques for CNT synthesis include laser ablation, discharge, and chemical vapor deposition (CVD) [42], as shown in Fig. 4. Arc discharge has proven an excellent method for producing high-quality MWCNTs [43] and SWCNTs [44]. In arc discharge, carbon atoms are evaporated using a helium plasma initiated by high currents passed through an opposing carbon anode and cathode. Thus, carbon

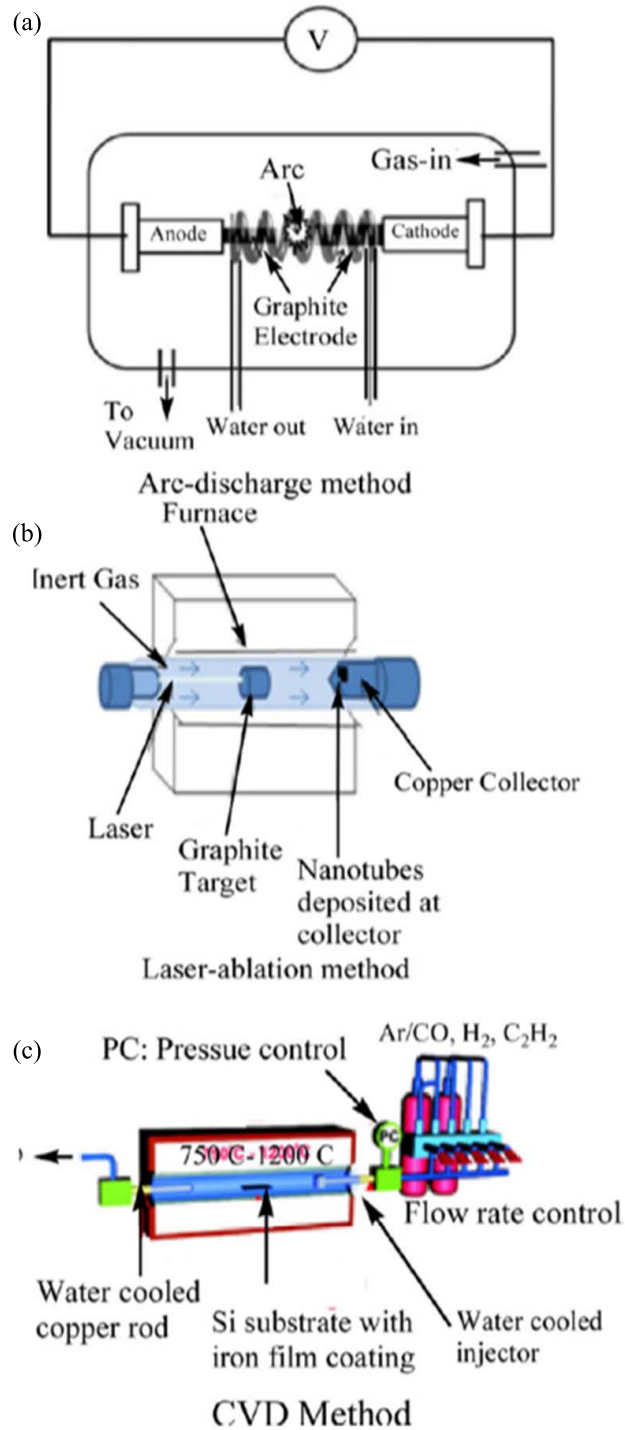

Fig. 4. Common CNT fabrication methods, including (a) arc-discharge method, (b) laser-ablation method, and (c) CVD method [42]. Figures reprinted with permission from [42] Copyright 2015, Taylor & Francis.

atoms can be generated from the evaporation of solid carbon sources to form CNTs. The temperatures involved in these methods are 3000 °C–4000 °C, close to the melting temperature of graphite. Usually, the anode is doped with a metal catalyst (i.e., Fe, Ni, Co, or Mo) to produce SWCNTs.

Laser ablation utilizes intense laser pulses to ablate a carbon target containing 0.5 atomic percent of nickel and cobalt [45]. Carbon atoms can be removed from a solid carbon source surface due to irradiation by the laser beam. Laser ablation involves pulsed laser deposition (PLD), a laser with a high-power density, and narrow frequency bandwidth to heat the carbon source for vaporizing carbon atoms to form CNTs. High-quality and high-purity SWCNTs can be grown using the PLD approach [46]. The fundamental differences between laser ablation and arc discharge are the methods to obtain carbon atoms; one is by high temperature from high currents, and another one is by high temperature from irradiating the laser beam. In laser ablation, a metal catalyst is not needed, and intense laser pulses are generated to deposit CNTs. Laser ablation is known to have a high production rate and yield.

Unlike these methods, CVD does not involve a bulk solid carbon source, such as graphite. Instead, a chemical reaction occurs to deposit materials on target substrates with a catalyst, induced by reactive gases, including carbon source gas(es), which continuously flows in a high-temperature furnace. Often, CNTs are synthesized via the reduction of carbon precursor by hydrogen on the substrate (such as Si) with a catalyst layer (such as Fe) [47]. The substrate typically contains a metal catalyst layer, and the carbon source gases react at its surface to deposit CNT coatings. The CVD method is characterized by enhanced alignment, with a location control down to the submicrometer scale, by metal catalysis patterning on substrate surfaces [48], [49], [50]. CVD has been demonstrated to control CNT geometric properties by adjusting the growth recipe, resulting in CNTs of tailorable diameter and length [31]. The selection of metal catalyst species has also resulted in preferential growth of either SWCNTs or MWCNTs [51]. The metal catalyst layer is usually deposited on the substrate via sputtering, followed by subsequent etching and/or thermal annealing to induce catalyst nucleation.

III. CNT-Based Flexible Electrodes

A. CNT Deposition and Transfer

Combining flexible substrate with sensing electrode is the foundation of flexible and wearable sensors. In this section, we introduce several typical immobilization methods for CNTs on a common flexible substrate to form CNT-based flexible electrodes.

Adapting CNTs toward flexible sensors often requires incorporating CNTs on a flexible (often nonconductive) substrate to create functional electrodes for various sensing applications [52]. The incorporation of CNTs onto flexible substrates can be achieved via solution deposition or transfer of CVD growth. CNTs can be transferred onto partially cured PDMS substrates to maintain alignment and imbue flexibility [53], [54], [55], [56]. CNTs can also be transferred onto thermoplastic materials, such as polycarbonate (PC) substrates [57]. Furthermore, CNTs can be transferred onto substrates [58], such as on Cu foil as the substrate for graphene growth, resulting in flexible electrodes for pressure sensors [59]. In solution deposition, CNTs are often randomly oriented and entangled together to form a disordered film on a substrate. In contrast, vertically aligned CNTs can be fabricated via CVD to form uniform carpets. For this reason, alignment achieved via CVD-grown CNTs often results in CNT-base electrodes that outperform solution-processed CNTs in electrical performance [60], [61]. CNT carpets are electrode surfaces composed of arrays of CNTs, in which neighboring CNTs entangle with one another due to van der Waals forces; these electrodes are characterized by low weight and ultrahigh strength with exceptional electronic and thermal properties [31], [32]. Solution deposition generally corresponds to randomly oriented tangled CNTs, known to clump within solutions via attractive van der Waals forces. This CNT deposition method is often used in industrial applications, as it allows scalability for high-yield and low-cost production and patterning via solution-based printing for localized control of deposition. CNTs synthesized by laser ablation or arc discharge often first go through preprocessing stages to purify CNTs by removing by-products of amorphous carbon and fullerenes. Ultrasonication methods are often used to resolve agglomeration issues associated with CNTs dispersed in solutions, but ultrasonication has been shown to introduce CNT defects [62]. To circumvent this problem, as-grown CNTs can be transferred directly onto desirable substrates.

CNT-based electrodes for sensors are often fabricated by solvent dispersion of CNTs that are immobilized onto a substrate. This process generally consists of two steps. Fabricated CNTs first undergo purification and activation pretreatments, followed by dispersion into solvent via sonification. Once properly dispersed, CNTs are printed onto a substrate via drop-casting, followed by drying. An extensively used solvent is *N*-dimethylformamide (DMF) due to its high solubility and exfoliation efficiency. Compared to other solvents, DMF has demonstrated superior dispersion properties [63]. In order to further enhance the solubility of CNTs, some additives can be added to the solvent to assist the dispersion of CNTs, including Nafion [64], surfactants [65], chitosan [66], polyethyleneimine [67], and sel-gels [68].

The most common approach of self-assembled immobilization is achieved by the presence of water-soluble polyelectrolytes on the sidewall of CNTs. Because of polyelectrolytes, arrays of CNTs easily attach to form a uniform structure. The molecular design of strong SWCNT/polyelectrolyte multilayer composites was reported previously [69]. Another approach to realize self-assembled immobilization takes place during the acid treatment of CNTs. In this method, negatively charged carboxyl groups introduced to the sidewalls cause CNTs to immobilize onto substrates. Assembling carboxylic terminated CNTs on an amino-terminated silicon surface was accomplished via electrostatic interaction. Carboxyl-terminated CNTs were also organized on gold substrates with a perpendicular orientation via a wet chemical self-assembling technique [70].

Another common method of immobilizing CNTs on an electrode surface involves the electropolymerization of various monomers in the presence of dispersed CNTs via electrochemical methods. During electropolymerization, CNTs are grown on surfaces of CNTs in the presence of ions or dopants during the electropolymerization process. Recent studies have demonstrated the electropolymerization immobilization method [71]. A conjugated organic dye—azocarmine B(ACB)—immobilized CNTs on a carbon glass electrode surface, resulting in excellent electrochemical sensor performance.

B. CNTs With Elastomer Polymers as Flexible Electrodes

The elastomer polymers typically show high viscosity and elasticity, especially high failure strain compared with other materials, making them the most common flexible substrates for flexible and wearable devices. Here, we introduce the performance of CNTs/elastomer polymer composite electrodes.

To imbue flexibility for CNT-based electrodes, the most common substrate materials include polymers, especially elastomeric polymers. Though CNTs independently may lack flexibility, the combination with flexible polymers allows the whole device to be flexible. Elastomeric polymers have been combined with CNTs as electrode materials [72], using a mixture of polymer and CNTs to minimize the slip between adjacent individual CNTs. Many other polymers have been used in flexible electrochemical sensors, such as thermoplastics [73], thermoset resins [74], and elastomers [75].

The transfer method of CNTs onto flexible substrates can directly influence the performance of CNT-based flexible sensors. CNTs on Si substrates were immersed in partially cured PDMS, and Si substrates were then removed, resulting in the full transfer of vertically aligned CNTs on PDMS [76]. Furthermore, deposition techniques were demonstrated by depositing dispersed CNTs on a flexible substrate, allowing complicated multilayer structures. A tissue paper/CNT-based flexible pressure sensor was developed by direct immersion in CNT solution to achieve CNT/tissue paper films [77]. CNTs were also dispersed in precured PDMS liquid for micromolding [78]. CNT/flexible polymer composites were furthermore obtained by directly coating PDMS on CNT films [79]. An ink printing technology was also used in CNT transfer, demonstrating highly stretchable fully printed CNT-based electrochemical sensors [80]. CNT ink was printed on a polyurethane (PU) flexible substrate to withstand high strains (up to 500%) at 2°. In addition, CNT-based flexible pressure sensors were fabricated using ink printing technology [81], where the printed CNT ink was used as an electrode layer.

CNTs are commonly deposited or embedded onto flexible or stretchable elastomer polymer substrates, such as polyethylene terephthalate (PET), PC, or polydimethylsiloxane (PDMS) [36], [55], [82], [83], [84], [85], [86], [87]. Combining these polymers with CNTs enables electrode materials with desirable electronic properties for energy storage and sensor applications. Electrodes composed of elastomeric substrates with CNTs have been demonstrated with the flexibility of 100% or greater [86], [88], [89], [90], [91], [92], with a limitation of the cohesive fracture of the elastomeric material. The resistance of CNT electrodes is shown to change as a function of the strain [55], [92], [93], [94]; conducting spray-deposited films of SWCNTs on PDMS substrate demonstrate a conductivity of 2200 $S \cdot cm^{-1}$, and the film accommodates strains up to 150% [95]. Fig. 5 shows the resistance change during applied strain and relaxation.

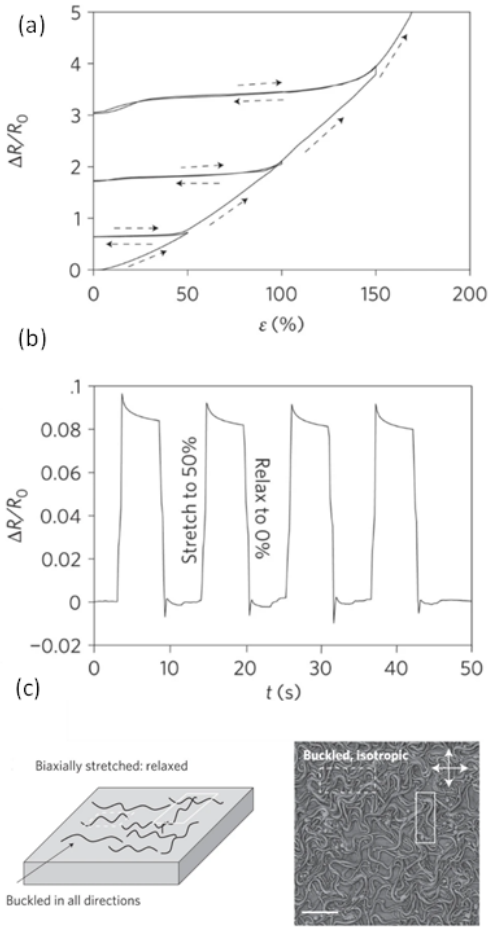

Fig. 5. Change in resistance versus strain for CNT film on PDMS substrate. (a) Change in resistance versus strain for the CNT film on PDMS substrate. (b) Cycling test for films stretched to 50%. (c) Schematic and AFM image of buckled CNT film on PDMS [95]. Figures reprinted with permission from [95] Copyright 2011, Springer Nature.

Flexible electrodes consisting of PDMS layers combined with CNTs have been pursued in various strategies to imbue sensing capabilities. PDMS is favorable for flexible electrode designs due to its transparent nature, notably high flexibility and mechanical robustness. Additional properties make PDMS an ideal choice for diverse biological applications due to its biocompatibility, chemical inertness, ease of synthesis, and low cost. For example, wearable patch devices have been used for the detection of human motion with various postures and moving speeds via a strain sensor fabricated with a flexible PDMS substrate with successive layers of SWCNT and poly(3,4-ethylenedioxythiophene) polystyrene sulfonate (PEDOT:PSS) inks [96]. The PDMS substrate acts as an adherent platform for sensing layers of the stacked piezoresistive nanohybrid film consisting of SWCNTs and a

conductive elastomeric composite of PU-PEDOT:PSS, which detects underlying strains on the user's face and enables the identification of subtle human emotion physical manifestations, including crying and laughing; due to the stacked three-layer design with PDMS as the bottom substrate, this wearable e-skin sensor demonstrates high stability, stretchability up to 100%, and optical transparency of 62%. PDMS has also been used in a skin-attachable strain sensor as a flexible substrate coated with conductive films containing MWCNTs and PEDOT:PSS, demonstrating high sensitivity, high durability, fast response, and high transparency [97]. Furthermore, PDMS was incorporated with CNTs toward a transparent sensor with PANI nanofibers and V_2O_5 on indium–tin-oxide-coated PET film, exhibiting an optical visual change in color according to the intensity of strain toward real-time sensing of body motion.

A significant benefit of elastomeric polymers, such as PDMS as a substrate, is its versatility due to its moldability, which allows PDMS to be cast into desirable geometries and surface morphologies. A flexible CNT-based strain sensor has been fabricated with a patterned PDMS substrate and combined with a PANI layer for dual functionality as a supercapacitor [98]; the PDMS is cast into a mold with a plant leaf surface and coated with aligned CNTs coated with PANI. The natural grooves and wrinkles in the leaf template introduce a patterned microstructure that exhibited higher performance than a conventional PDMS substrate counterpart. The patterned microstructure reduces the spacing between CNTs, allowing greater connections when undergoing strain. As a result, a larger range of detectable strain is observed as a flexible strain sensor, greater than 40% compared to the nonpatterned PDMS substrate.

IV. CNT-Based Flexible Electrochemical Sensors

Flexible sensors can be divided into two categories: flexible mechanical sensors and flexible electrochemical sensors. In this section, we discuss flexible electrochemical sensors first, starting by introducing the working principle of CNT-based electrochemical sensors and discussing the applications.

Electrochemical sensors can detect electrochemical reactions via interaction between the sensing surface and the analytes [99]. CNTs have excellent electronic and chemical properties due to their unique nanostructures, providing highly desirable characteristics, such as large surface area, excellent conductivity, and good biocompatibility. Thus, the application of CNTs on electrochemical sensors has been intensively explored.

Individual CNTs have a nanotube structure with two distinct surface regions: the sidewalls and ends. The sidewall regions of congregated CNT forests can provide a larger surface area (large surface-to-volume ratios) than graphene, increasing reaction sites. Pertaining to a low volume, CNTs can also be used in microelectronic devices. Moreover, CNTs have been found to enhance the electrochemical reactivity of major biomolecules and proteins [100], [101]. To explore the application of electrochemical sensors based on CNTs, it is essential to analyze the fabrication methods and working mechanisms, including substrate selection, immobilization method, functionalization method, and the arrangement of CNTs.

Another direction for exploration to expand the application field of electrochemical sensors is imparting flexibility to create flexible electrochemical sensors. The size of the device and the ability to resist deformation caused by chemical or physical factors are two major factors for consideration. Electrochemical sensors based on CNTs realize miniaturization, allowing the effective shrinking of wearable devices to impressively small and discreet units [102]. Furthermore, with the development of flexible materials, highly desirable electrochemical sensors can be realized by combining CNTs and flexible substrates, resulting in excellent conformability, high flexibility, and seamless daily life integration.

A. CNT Functionalization

The unique chemical structure of CNTs allows several functional groups to be attached to the surface. Thus, the functionalized CNTs can be applied in the electrochemical sensing area. In this section, we show three primary functionalization methods of CNTs.

An effective means to expand the applications of CNTs is through their functionalization. Although CNTs have many unique properties that bestow these materials with significant potential to be used in various electrochemical sensors, the sidewall region of pristine CNTs is chemically inert. Functionalization can solve this problem; it is crucial for fully exploiting CNTs for diverse applications. Researchers have developed effective methods to functionalize CNT surfaces, such as polymer wrapping, biomolecule binding, and metal ion binding. To further enhance the chemical sensitivity of CNTs, other functionalization routes have been developed in the past few years, including chemical and solid-phase or hydromechanochemical methods [103].

Noncovalent functionalization of CNTs, characterized by noncovalent bonding of functional groups directly on CNT surfaces is commonly accomplished by an oxidative process of CNTs, producing defects located on the sidewall. These defects create spaces for other functional groups to be anchored on the CNTs, providing chemical reaction sites. However, this method is hard to control, and too many defects will weaken the electrical properties of CNTs. Therefore, a new noncovalent functionalization method, known as the small-molecule-based noncovalent functionalization method, has been reported to expand the application area. In this approach, the dissolution and the surface modification of SWCNTs are achieved using a commercially available diazo dye, Congo red [104], which results in very stable performance. There are several derivative methods, including biomolecule-based noncovalent functionalization [105].

Covalent functionalization of CNTs is an additional method that has been employed in the literature [106]. In addition to noncovalent bonding, the functional group can be combined with CNTs via covalent bonding. For example, Williams *et al.* [107] developed a method to couple SWCNTs covalently to peptide nucleic acid (PNA, an uncharged DNA analog) and hybridized these macromolecular wires with complementary DNA. Covalent functionalization can create

a stronger bond between functional groups and CNTs, contributing to higher durability and long-term use.

Conjugated polymers, such as polyaniline, polypyrrole (PPy), polythiophene, and their derivatives, can be combined with CNTs as promising materials for electrochemical sensors [103]. In combination with conjugated polymers, interactions between CNTs and polymers containing large molecules with functional groups can be covalent, electrostatic, hydrogen bonding, and/or π-stacking. The strong chemical interaction of polymers and CNTs leads to strong components coupling, pertaining to higher sensitivity and sensor response, especially in flexible sensors that rely on high connectivity when undergoing repeated mechanical strain. A chemical polymerization of pyrrole monomer on MWCNTs can be achieved without adding any oxidants at room temperature [108]. Compared to noncovalent functionalization methods, this method can bypass the requirement of lower temperatures and reduce the introduction of other impurity ions common with the oxidants used in the oxidative method. Furthermore, the polymer functionalization treatment can preserve the integrity and the electronic structure of CNTs, as it produces fewer defects.

B. Glucose Sensors

Glucose biosensors increasingly draw attention owing to the requirements of patients with diabetes. The flexible CNT-based glucose sensors can be combined with monitor systems to realize real-time sensing. In this section, we discuss the applications of CNTs in flexible glucose-sensing areas.

Electrochemical glucose sensors can be categorized into two types: enzymatic and nonenzymatic sensors [109]. Enzyme sensors composed of modified glucose oxidase are widely used for glucose determination. However, enzymes can be sensitive to variations in environmental conditions, and there are some other drawbacks to using enzymes, such as high price and low stability [110]. To resolve these problems, nonenzymatic sensors based on CNTs have recently been investigated.

An electrostatically functionalized MWCNT-based flexible and nonenzymatic biosensor has been developed for glucose detection [111]. The nonenzymatic glucose sensor was based on electrostatically functionalized MWCNT electrodes, followed by thermally embedding the electrode in a flexible substrate to obtain a flexible glucose sensor. The electrostatic functionalization method has also been developed [112], in which the high electrical field ionized the oxygen, absorbed onto the surface of CNTs to form oxygenated functional bonds. This flexible glucose sensor can be fabricated easily, but there are limitations with the sensitivity to detect glucose. In comparison, glucose sensors based on CNT-FETs have shown a greater sensitivity. This type of sensor operates by an electrical signal produced when the resistance changes due to the absorption of glucose molecules on the FET surface, which are highly sensitive. Fig. 6 shows a diagram of a CNT-FET glucose sensor [113]; Fig. 6(a) shows the PDDA-SWCNT hybrid structure combined with PET polyester flexible substrate to form a flexible sensor, and Fig. 6(b) shows the working mechanism. The glucose oxidase accumulates on the surface of CNTs to change resistance in the presence of glucose, resulting in a detectable electrical signal.

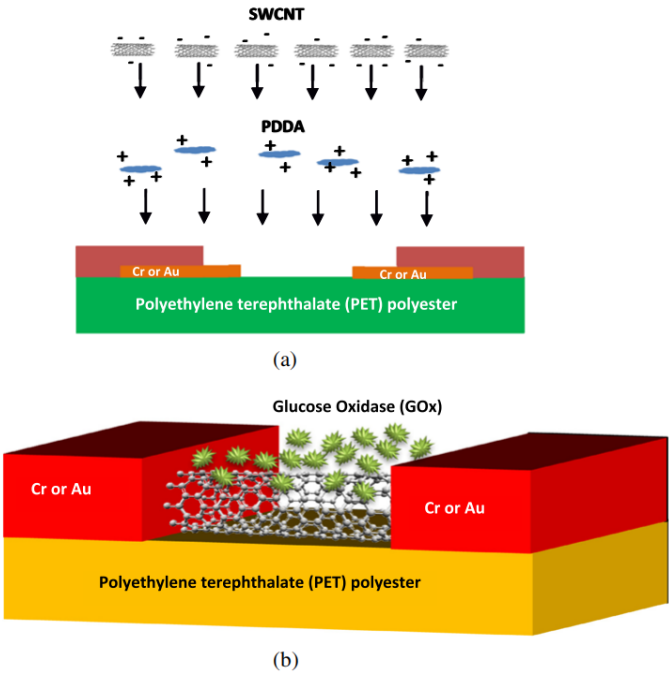

Fig. 6. Schematics of a field-effect glucose sensor. (a) Schematic of the fabrication process of the glucose sensor [175]. (b) Proposed combination of metal electrodes made of chromium or gold, a layer of glucose oxidase biomolecular assembly, and SWCNT channel in the form of FET. Figures reprinted with permission from [175] Copyright 2014, Springer Nature.

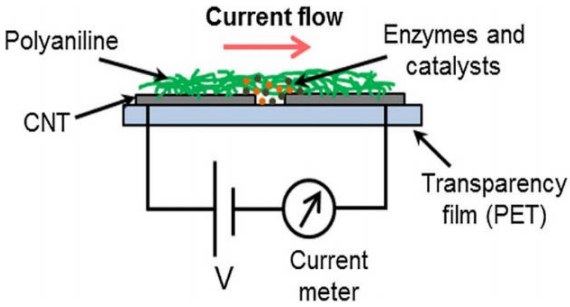

Fig. 7. Chemiresistive sensing configuration based on two CNT carpets and polyaniline nanowires [251]. Figures reprinted with permission from [251] Copyright 2016, Springer Nature.

Recently, the flexibility of the CNT-based glucose sensors has been developed further to achieve a wearable glucose sensor based on CNTs. Still, the demand for glucose sensors is often closely coupled with insulin delivery since insulin often needs to be delivered into the bloodstream. Therefore, microneedle technology continues to be developed, such as through microneedle-based self-powered glucose sensors [249]. A skin-attachable, stretchable electrochemical sweat sensor has been reported for glucose and pH detection [114]. Compared to conventional glucose sensors, it is wearable, noninvasive, and highly sensitive. Traditional glucose sensors require the use of blood, and the detection of blood glucose levels is usually invasive with complications

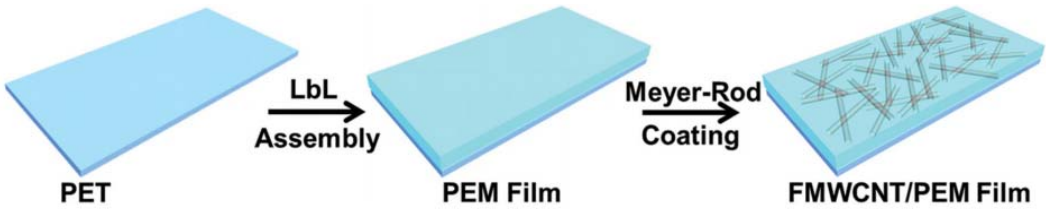

Fig. 8. Schematic illustration of the fabrication of CNT network-coated LbL-assembled transparent healable PEM films by effectively casting transparent CNT networks on self-healing substrates [117]. Figures reprinted with permission from [117] Copyright 2015, Wiley Online Library.

including skin irritation and discomfort. Therefore, wearable glucose sensors detecting glucose in alternative bodily fluids, such as sweat, have recently been pursued. Skin-attachable glucose sensors can be desirable for diabetic patient care, and they can monitor glucose continuously.

In addition to electrochemical glucose sensors, the chemiresistive glucose sensors are also trending in this research area. With the development of nanomaterials, the resistance of some materials shows high sensitivity to chemical environments, such as pH [250]. Therefore, by measuring the resistance of sensing materials with a chemical reaction, one can monitor the concentration of the chemical analyte. For example, polyaniline can be combined with CNTs as the sensing material to constitute a CNT-based chemiresistive glucose sensor [251], as shown in Fig. 7. Here, polyaniline is a conducting polymer whose conductivity is highly sensitive to its chemical surroundings. By employing these unique properties, this glucose sensor can monitor the glucose concentration by measuring the pH variation during glucose oxidation.

C. Healable Gas Sensors

Flexible and even self-healable gas sensors are meaningful for many areas. In this section, we list the applications of CNTs on flexible and healable gas sensing areas.

The need for sensing gases arises from many fields, including fire control, atmospheric research, and medical analyses. Typically, the gas sensor is a bulk instrument, and it does not meet daily use. CNT-based devices with various gas sensing mechanisms have been used to develop small-scale gas sensors [115]. The interaction of gases with CNTs at the contact area of metal-CNT is the major factor determining the sensitivity. The current change resulting from natural adsorption can be relatively weak. However, when attaching CNT to a gold nanowire, the electrical signal is amplified up to 30%. Detection of gases via electrochemical sensing with a field-effect transition has reported a p-channel FET to detect oxynitride [116].

The development of flexible gas sensors for fire control and atmospheric research demonstrated a flexible and healable gas sensor based on MWCNTs' network-coated polyelectrolyte multilayer film [117]. Fig. 8 shows the fabrication process of CNT network-coated layer-by-layer (LbL) assembled healable PEM films. Fig. 9 shows the working mechanism of the healable characteristic.

D. Metal Sensors

Metal sensors are one of the most common electrochemical sensors. In this section, we introduce the meaning of flexible metal sensors and the applications of CNTs.

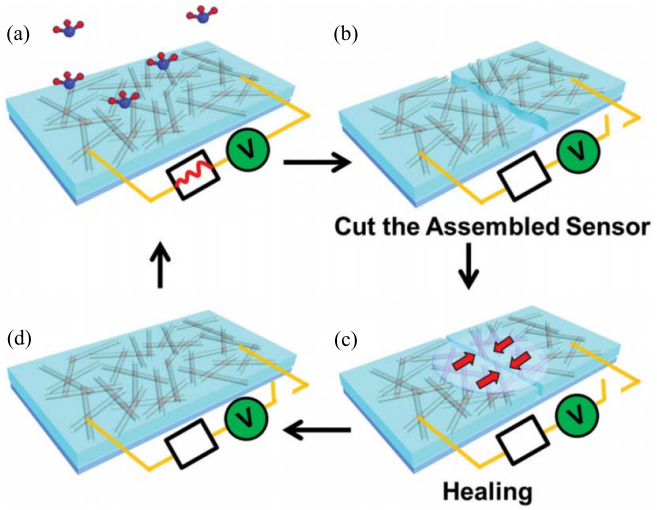

Fig. 9. Working mechanism of the healable gas sensor: (a) effective sensing from the assembled healable transparent chemical gas sensor, (b) cutting of the assembled sensor, (c) water-enabled healing, and (d) after healing [117]. Figures reprinted with permission from [117] Copyright 2015, Wiley Online Library.

In the past, heavy metal ion sensors were mainly applied for environmental protection, and thus, flexibility and miniaturization were not considered [118]. However, the application of heavy metal detection has expanded beyond environmental, and attention has been focused on their use for food analysis [119], [120]. In addition, many heavy metals are harmful to human health, such as lead, cadmium, and arsenic [121]. Therefore, the low-cost and high-sensitivity electrochemical sensors for heavy metal sensing are in great demand, and flexibility and miniaturization have become significant for these applications [122].

CNT-based heavy metal sensors have been realized via reduced graphene oxide-CNT (rGO-CNT) as a miniaturized flexible sensor [54]. rGO-CNT composites were also patterned into Au/rGO-CNT electrodes on the flexible PI substrate via microfabrication [55]. After the deposition of bismuth film on the surface of the electrode, a sensor with three electrodes for the detection of lead and cadmium ions can be integrated [55]. Fig. 10 shows that the rGO-CNT composite can improve the sensitivity significantly [54].

In addition to lead and cadmium ions, other heavy metal sensors based on CNTs have been realized by different functionalization methods. Paul *et al.* [123] have demonstrated DNA functionalized CNT to detect Hg(II) ions over Cd(II) and Pb(II) ions. The nucleobases of DNA, such as adenine and thymine, can be bound to the surface of CNTs through

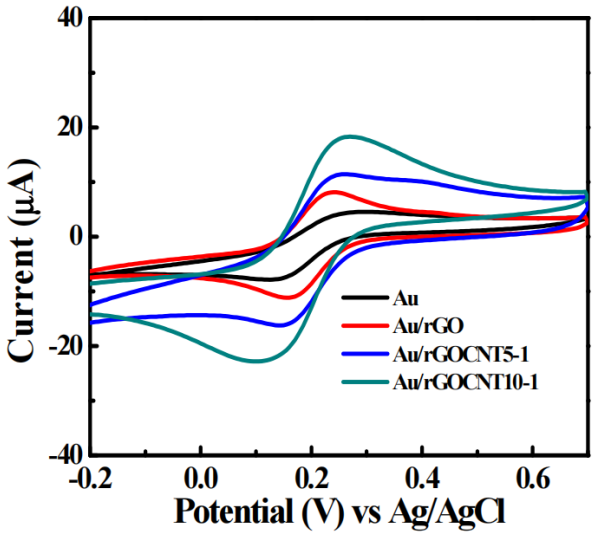

Fig. 10. Cyclic voltammogram of different working electrodes. Au electrode (black line), Au/rGO electrode (red line), Au/rGOCNT5-1 electrode (blue line), and Au/rGOCNT10-1 electrode (green line) [176]. Figures reprinted with permission from [176] Copyright 2017, IEEE.

π–π affinities for Hg(II) ions and can attract Hg(II) ions to form a stable structure. The coordinate ligand-Hg(II) bond possesses a higher covalent character than either the ligand-Cd(II) or ligand-Pb(II) bond. Therefore, it can precisely detect Hg(II) ions over Cd(II) and Pb(II) ions. Lien *et al.* [124] also provide a green functionalization method for CNT to fabricate lead ion sensors. A Nafion-modified graphene/CNT composite deposited with Bi on the screen-printed electrode has been realized to replace the traditional Bi film method to detect lead ions. The result shows that the sensitivity of lead ions on Nafion-G/CNT-BiSPE was about 50 times higher than the traditional method of stacking interactions. The larger surface area provided by CNT can help enhance the reaction area. Combining functionalized CNTs with the flexible substrate can be used for multiple kinds of heavy metal sensors that are both flexible and wearable.

E. Implantable Biomedical Sensors

Flexible and implantable biomedical sensors are meaningful for the health-monitoring area. In this section, we show the performance of CNT-based flexible and implantable biomedical sensors.

Cell interfacial sensors are used to detect the molecular release of cells, primarily used in biomedical areas, such as vital signs (i.e., glucose, blood fat, and blood platelet) and cancer cells, which can help to monitor various indicators, especially for cancer/leukemia patients, with faster response times and with greater convenience. The flexible and miniaturized cell interfacial sensors based on CNTs have been developed to make the sensor skin-attachable or body-implantable.

For *in vitro* bio-microsystems, the novel porous membrane-based biosensors were developed [125], resulting in high sensitivity, resulting in high sensitivity on the scale of cell-molecular release by directly detecting low quantity levels. The porous membrane-based biosensors are operated via membrane-integrated cyclic voltammetry (CV) with a CNT-modified working electrode and were shown to selectively detect neurotransmitter serotonin (5-HT). Fig. 11 shows the whole structure with a demonstration of its flexibility. In addition, this membrane can support cell-interfacial impedance electrodes to monitor complex body signals. In the future, this approach can directly be used to fabricate additional biomedical sensors with diverse applications.

In addition to cell-interfacial sensors, implantable biomedical sensors can help detect low concentration bioindicators inside the body, an important index to evaluate disease severity. A bioindicator, chondroitin sulfate proteoglycan (CSPG), is the main component of the glial scar, which will inhibit axonal regeneration after spinal cord injury. Jeong *et al.* [126] have developed a highly flexible and implantable electrochemical biosensor as a substitute for magnetic resonance imaging (MRI) to monitor glial scar, resulting in high sensitivity and low cost. COOH-functionalized MWCNT networks were deposited on a flexible polymer substrate to fabricate the sensor. The large surface area of CNTs provided a large reaction region for low concentration conditions. The minimum concentration at which CSPGs inhibit axonal regeneration was about 10 μg/mL. This kind of CSPG sensor can detect CSGPs at the concentration of 1 μg/mL, proving that it can precisely detect CSPG even in very low concentrations.

F. Pathogen Diagnosis

Rapid pathogen diagnosis by sensors is a novel area. In this section, we focus on the performance and structure design of CNT-based flexible pathogen sensors.

Flexible electrochemical sensors based on CNTs have two major advantages: high sensitivity and miniature size, owing to their novel development focusing on diagnosing pathogens and wearable electronics. An HIV DNA biosensor based on CNTs has been developed with flexibility. The sensor is based on a flexible paper-based Ni-MOF composite/AuNP/CNT film electrode to detect HIV DNA directly [127]. The Ni-MOF composite/AuNPs (Ni–Au composite) are deposited on the surface of the CNT/PVA film electrode to form Ni–Au composite/CNT/PVA (CCP) film, and CNTs are provided a large reaction surface to load a large amount of single DNA for HIV detection. In addition, the paper-based structure enabled high flexibility. Fig. 12 shows the fabrication process of this film. The result shows that the paper-based sensor could maintain stable performance even having been after 200 times bending or 0%–20% stretching under different strain conditions. Thus, the CNT-based electrode successfully detects HIV DNA even in a complex chemical environment.

For wearable electronics, the detection of sodium in sweat can help monitor health metrics during sports or fitness. The major challenge for a wearable sodium sensor is maintaining stable performance under inevitable mechanical deformation and good electrochemical properties under the erosion of sweat. A fully flexible sodium sensor system with integrated Au/CNT/Au nanocomposites has been developed [128]. Fig. 13 shows the whole structure and the flexibility of this sodium sensor. Lim *et al.* [128] have

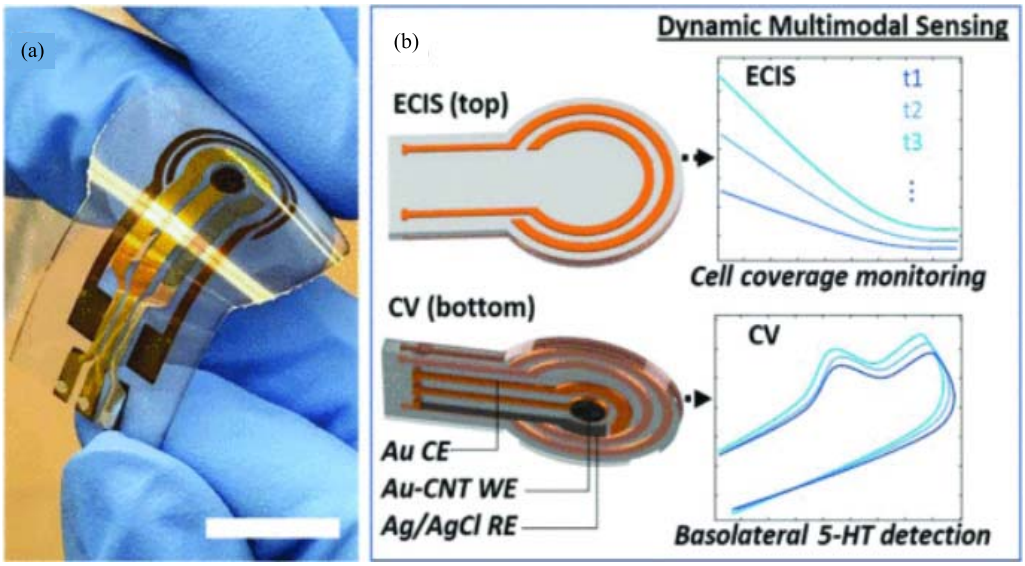

Fig. 11. Multimodal electrode-integrated porous cell culture membrane. (a) Image of electrodes fabricated on a transparent, flexible membrane. Scale bar = 10 mm. (b) Diagram of multimodal electrode functionalities. CE, WE, and RE: counter, working, and reference electrodes [125]. Figures reprinted with permission from [125] Copyright 2019, IEEE.

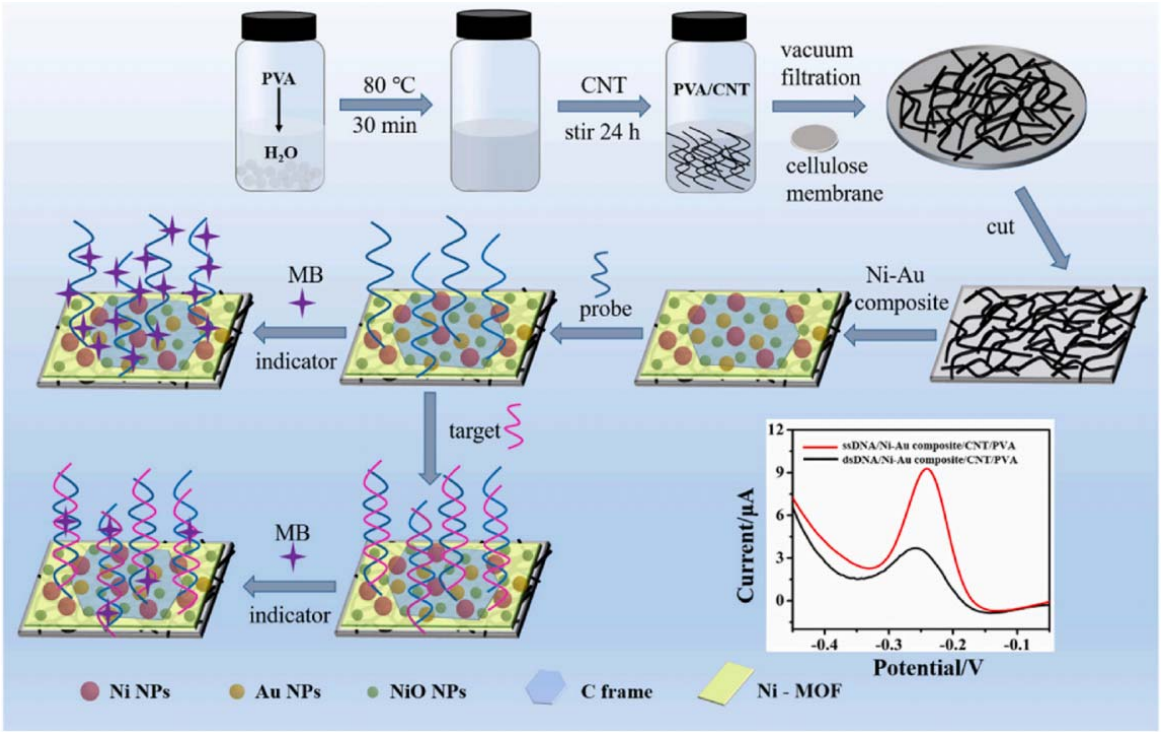

Fig. 12. Schematic of the fabrication process for the flexible Ni–Au composite/CNT/PVA film electrode and the detection of the target DNA [127]. Figures reprinted with permission from [127] Copyright 2021, Elsevier.

also demonstrated the performance comparison between this sensor and various similar products; the flexible sodium sensor demonstrated higher sensitivity compared to other rigid bulk electronics in addition to a minimum volume with a low-performance variation of only roughly 3% when it is attached to the skin during continuous motion.

V. CNT-Based Flexible Mechanical Sensors

Flexible Mechanical sensors are another category. This section introduces the development of CNT-based flexible mechanical sensors and then lists several applications and discusses how CNTs help enhance mechanical sensing performance.

Mechanical sensors are made to be sensitive to changes in mechanical stimuli, including strain, force, and pressure. Detection of mechanical properties has been employed for healthcare monitoring [129], robotics [5], civil engineering [23], electronic skins [130], aerospace [131], and human–machine interfaces [132]. Mechanical sensing often detects deformation, translated into a recordable electrical signal and undergoes signal processing.

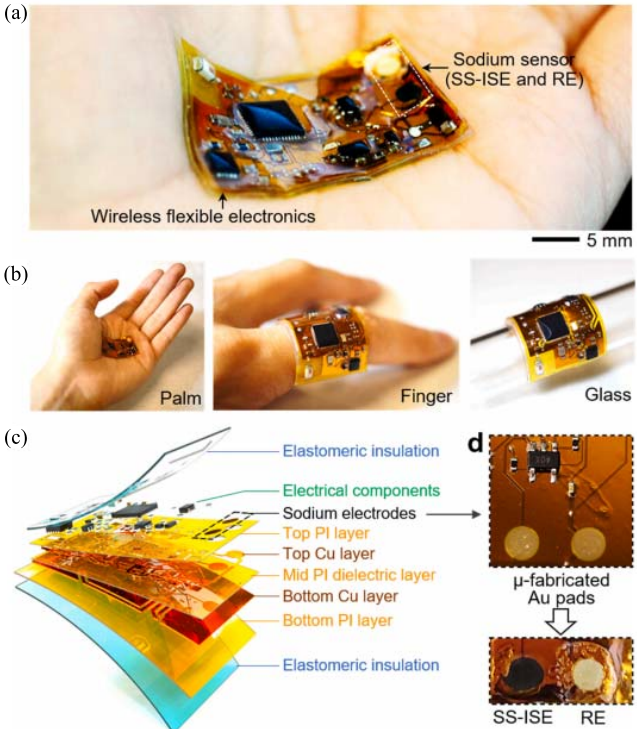

Fig. 13. Overview of an all-in-one, wireless, fully flexible sodium sensor system. (a) Photograph of an integrated, flexible device composed of a thin-film sodium sensing SSISE, reference electrode (RE), and wireless membrane circuit with integrated functional chips for data acquisition. (b) Photographs capturing the seamless integration of the device on a palm, a finger, and a glass bulb. (c) Multilayered integrated device fabricated by using the combination of microfabrication, hard-soft material integration, transfer printing, and electrochemical deposition. (d) Sodium sensor composed of a pair of thin-film SS-ISE and RE on μ-fabricated Au pads [128]. Figures reprinted with permission from [128] Copyright 2021, Elsevier.

A force sensor can be used to measure tensile, compressive, shear, torsional, bending, and/or frictional forces. A touch sensor is a force sensor specifically used to measure contact of an approaching force (i.e., object) to the sensor surface. An ordered array of touch sensors can be incorporated within a design to fabricate a tactile sensor, which is used to measure the spatial distribution of forces to the sensor surface. Tactile sensors are often used in robotics applications to simulate the complex sensation of touch toward the detection of a variety of surface properties, including texture, shape, and hardness [21], [130], [133]. The resulting response of a flexible electrode to applied mechanical stimuli identifies the type of mechanical sensor that can be realized. Applied strain to an electrode can be correlated with a change in resistance, defined by the relationship between the change in geometric/mechanical alterations due to applied strain and the resulting change in conductance. This behavior allows measuring changes in resistance of a conducting material toward strain sensing applications. Mechanical sensors operate via the detection of acoustic waves that respond to the propagation of these mechanical waves across the sensor's surface that alters with wave properties, including amplitude and velocity. Inertial sensors, including accelerometer and gyroscope, can sense acceleration and angular acceleration, respectively. Piezoresistive sensors respond to pressure, bending, or force and contain piezoelectric materials that produce an electrical charge proportional to an applied force [134]. With the application of mechanical load, a resistance change occurs, which is detectable by the sensors. Mechanical sensors exist in various forms and are synthesized to sense desirable mechanical characteristics of a system.

Recently, CNTs have been explored as components for developing flexible mechanical sensors. CNT ribbons have been directly drawn from CVD-grown CNTs, such as stretchable electrodes with a high aspect ratio, high conductivity, and mechanical toughness [135]. CNTs realized in flexible electrode designs are often incorporated as functional fillers within polymer materials [136]. Electrically conductive conjugated polymer coatings on CNTs were also demonstrated for mechanical sensing, such as polymer-coated CNTs [137].

A. Wearable Applications

This section lists several typical CNT-based mechanical sensors, followed by the introduction of the structures and the discussion of the working principle of those sensors.

Various wearable and flexible mechanical sensors have been realized with CNTs with flexible polymers to form flexible conductive electrodes that detect various forms of human motion. A flexible strain sensor has been realized through a facile and low-cost leaf templating process to pattern PDMS incorporated with wrinkled CNTs as a conductive layer that records changes in resistance due to the application of strain [98]. As shown in Fig. 14(a), human motion at one's joints has also been recorded by strain sensors comprised of CNTs embedded in transparent polymer films [138]. Large-scale human motion monitoring sensors have also been demonstrated with hydrogels composed of CNTs, including finger motion and bicipital muscle of arm motion, as shown in Fig. 14(b) [139]. A flexible capacitive pressure sensor has been used for gait signal analysis via nylon filter paper-based MWCNT and PEDOT:PSS composite electrodes and flexible PDMS layers [140]. Wound dressing applications have also been realized by combining CNTs and PPy coatings on conventional PU elastomers to form flexible and antibacterial piezoresistive porous devices that detect human motion [141].

Flexible skin-attachable CNT-based sensors have been realized to detect subtle human motion in response to mechanical stimuli. As shown in Fig. 14(c), stacked PU-PEDOT:PSS/SWCNT/PU-PEDOT:PSS structures were used to detect sensitive measurements relating to facial motions, including emotional expressions of crying and laughing [96]. Similarly, PANI/nickel nanoparticles (Ni NPs) /COOH-functionalized MWCNTs (COOH-MWCNTs) conductive paste has been incorporated on cotton fabric as a flexible pressure sensor to detect additional subtle human micromotions, such as face, eye, and finger movements. Using a PU foam substrate, a skin-like stretchable array of mechanical sensors with coatings of MWCNT/PANI nanocomposite was demonstrated toward subtle wrist pulse measurements, as shown in Fig. 14(d) [142]. CNTs have also been used in MWCNT-PANI composites as electrode materials in pressure sensor arrays to enable tactile sensing that mimics the sense

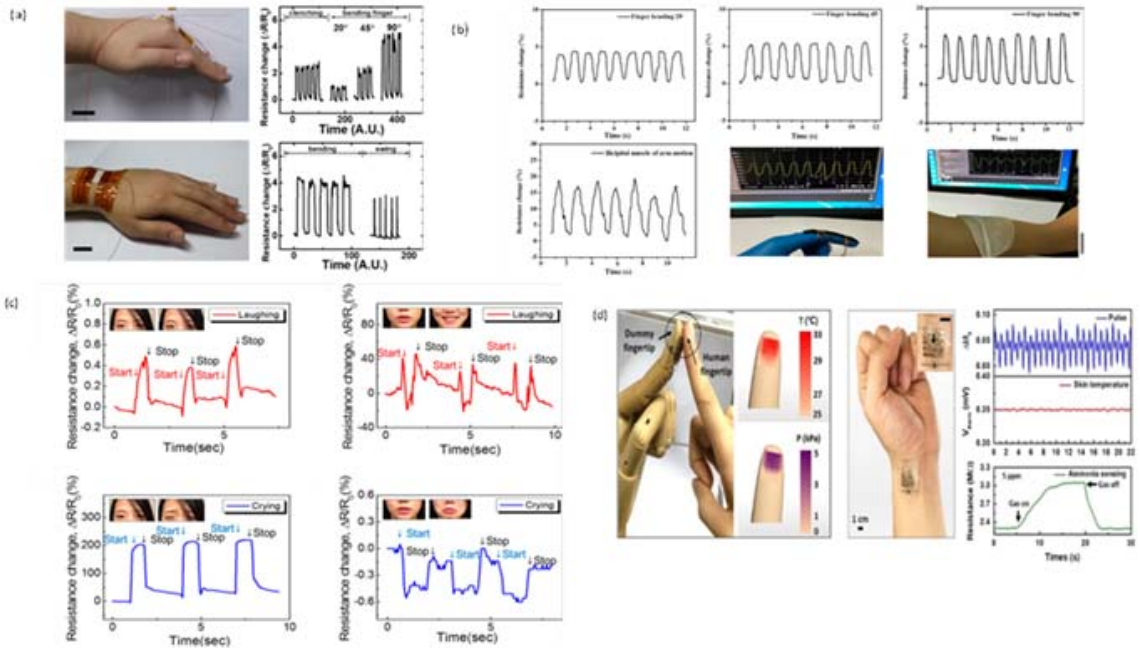

Fig. 14. (a) Strain sensor mounted on the knuckle (top left) and the backside of the wrist (bottom left) for detecting human motions: finger motions of clenching, bending with angles of 20°, 45°, and 90° (top right), and hand motions of bending, swing with a badminton racket (bottom-right) [138]. (b) Large-scale human motion monitoring sensors have also been demonstrated with hydrogels composed of conjugated polymers with CNTs, including finger motion and bicipital muscle of arm motion [139]. (c) Time-dependent $\Delta R/R0$ responses of the sensor attached to the forehead and skin near the mouth to detect facial motions, including emotional expressions of crying and laughing [96]. (d) Skin-like stretchable array of mechanical sensors based on PU foam coated with MWCNT/PANI nanocomposite was demonstrated toward subtle wrist pulse measurements [142]. Figures reprinted with permission from [138] Copyright 2018, IOP Publishing. Figures reprinted with permission from [139] Copyright 2018, ASC Publications. Figures reprinted with permission from [96] Copyright 2015, ACS Publications. Figures reprinted with permission from [142] Copyright 2017, Nature Publishing Group.

of touch with tunable measurement range and high durability. *In vivo* physiological monitoring has also been accomplished by an injectable conductive self-healing hydrogel, composed of MWCNT-PEDOT-PAM-PVA, which is cross-linked in a simplified process to achieve reliable detection of precise pulse signals from the human radial and carotid arteries [143].

In addition to flexible polymer-based electrodes, various fiber-like structures and e-textiles have also been developed toward wearable mechanical sensors for sensing a wide range of human motions. Cotton/CNT sheath-core yarn has been demonstrated on various parts of the human body to detect finger, wrist, and leg movement, in addition to more sensitive esophageal movements [144]. The durable CNT-based mechanical sensor has been demonstrated as a breathable textile that could withstand conventional textile washing methods [145]. A wearable and shape-memory strain sensor comprised of flexible thermoplastic PU fiber as the core support coated with well-aligned CNT has been shown to detect multimodal deformation (tension, bending, and torsion) with demonstrated applications of detection of finger bending, breathing, and phonation [146]. Additional e-textile sensors composed of stitchable CNT-based fiber sensors have been demonstrated toward force sensing via changes in resistivity upon application of force [147]. A sensor design of conventional textile (i.e., cotton fabric) coated with CNT and PANI was also demonstrated for pressure sensing with application toward wearable use [148]. CNT-based mechanical sensors in textiles widen their application toward wearable applications.

B. Durability

Flexibility and durability are two significant indicators to measure the performance of flexible mechanical sensors. This section discusses the antistrain performances of various CNT-based mechanical sensors and explains how CNTs can be used to enhance flexibility and stretchability.

Flexible mechanical sensors commonly appear in wearable applications, often exposed to strains, impact, and potentially harmful environmental conditions. Thus, durability toward repeated loads is important for flexible mechanical sensors in their implantation in real-world applications [129]. Many strategies have been pursued in the literature to fabricate and test CNT-based sensors that can withstand these forms of exposure. However, existing flexible polymer materials that are often combined with CNTs to create flexible mechanical sensors also have inherent limitations with tearing or damage. To compensate for these known limitations and expand their capacity, strategies have been pursued toward self-healing and protective properties to retain reliable sensor performance within expected practical environments.

Durable and highly flexible substrates have primarily focused on demonstrating durable and flexible platforms incorporated with CNTs toward flexible mechanical sensors. A porous PDMS structure to enable breathability has been used as an intermediate layer between CNT-based sensing layers. A capacitive pressure sensor to offer structure enabling high stability (>10 000 compression-release cycles) with a high $R2$ value of 0.97, and a wide working

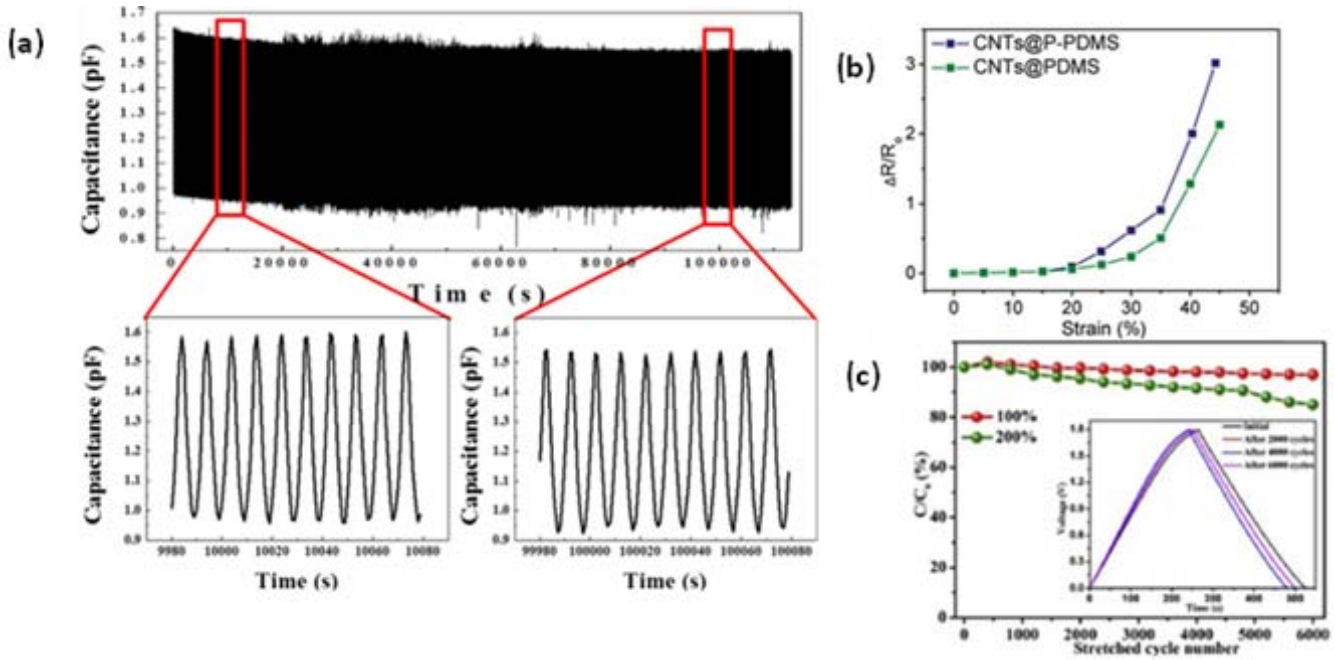

Fig. 15. (a) Reliability test of the fabricated sensor under the repeated 10 000 compression-release cycles at a frequency of 0.1 Hz [140]. (b) Increased durability of strain sensor design with a patterned PDMS substrate [98]. (c) Normalized capacitances of the pressure sensing device with stretching by 100% and 200% tested for 6000 cycles [150]. Figures reprinted with permission from [140] Copyright 2018, Elsevier. Figures reprinted with permission from [98] Copyright 2019, Wiley Online Library. Figures reprinted with permission from [150] Copyright 2020, Elsevier.

pressure range (<1200 kPa), as shown in Fig. 15(a) [140]. Due to its high stability, the wearable sensor is inserted into an insole and withstood mechanical stress caused by walking, enabling its use for real-time gait-signal monitoring. As shown in Fig. 15(b), patterning PDMS substrates with microstructures has also been pursued in CNT-based strain sensors to increase its durability under stretching when compared to unpatterned PDMS substrates [98]. High strain performance has also been observed with fiber substrate designs, such as cotton/CNT sheath-core yarn, which results in highly stretchable spring-like structures that exhibit excellent stability and an ultrahigh strain sensing range of 0%–350% [149]. Coaxial-fiber strain sensors composed of CNT have also exhibited durable and stable performance after stretching for 6000 cycles at a strain of 200%, as shown in Fig. 15(c) [150].

Protective coatings have also been employed within flexible CNT-based mechanical sensor designs. For example, a highly robust flexible textile sensor was developed with a layer of PPy-polydopamine-perfluorodecyltrlethoxysilane (PPy-PDA-PFDS) deposited on top of a CNT network transducer layer embedded on a textile substrate (i.e., simultaneously superhydrophobic and superoleophobic), protecting itself from the interference of a variety of agents and demonstrated reproducible performance following machine-washing and tape-peeling cycles [145]. PVA has also been used as an exterior coating on CNT-based flexible sensors to increase Young's modulus and additional environmental protection. Hui *et al.* [151] have performed a 2000-cycle fatigue test to demonstrate that the performance is relatively identical to the sensor without coating.

Tensile strain often leads to crack formation and propagation in conductive thin films, which can inhibit the performance of a flexible mechanical sensor [152]. Conjugated polymers have been combined with CNTs to offer enhanced electronic properties and mechanical robustness as films. A CNT-based piezoresistive motion sensor composed of CNT and PPy layers demonstrated high stability and reversible net-like microcrack formation under moderate stretching deformations. The CNTs act as electric bridges between microcracks observed in the polymer matrix [141]. Kim *et al.* [138] have introduced a fiber-reinforced region formed by inkjet-printing SWCNT thin films in a PEDOT:PSS thin film to demonstrate a strain sensor that suppressed crack propagation in fiber-reinforced regions under tensile strain. Even after 1000 cycles at 50% tensile strain, a working range of 70% is still observed, and the high performance is explained by different fracture mechanisms at the CNT-reinforced regions of the PEDOT:PSS films.

Crack formation is also mitigated by designing flexible mechanical sensors with self-healing properties. Self-healing hydrogels can repair and restore their original functionality when damaged by strain or impact [153]. This form of durability can increase the lifetime of a wearable sensor that is prone to tears and mechanical damage. For example, nanostructured PPy and CNTs have been incorporated into self-healing hydrogel sensors as multifunctional wearable pressure sensors [139]. Observations of its self-healing ability have been made by cutting the sensor into two distinct pieces and contacting the ends to allow unassisted self-healing; the resulting healed hydrogel is lifted by one end without observable boundaries, demonstrating its ability and efficiency. Similarly, an injectable self-healing hydrogel consisting of CNT and

TABLE I
COMPARATIVE TABLE OF CNT-BASED MECHANICAL SENSORS [59], [76], [77], [78], [79], [81], [157], [158], [159], [160], [163], [164], [178], [179], [180], [181], [182], [183], [184], [185], [186], [187], [188], [189], [190], [191], [192]

Publication Year	Target	Electrode Materials	Flexible Substrate	Operation Method	Flexibility	Sensitivity	Sensing Range	Addition Information	Durability	Reference
2013	Pressure	CNT / Au / Cr	Polydimethylsiloxane (PDMS)	Resistive pressure sensor based on CNT/PDMS flexible structure	-	-	0 - 200 kPa	-	-	[76]
2015	Pressure	CNT / Graphene	Thermoplastic polyurethane (TPU)	Resistive pressure sensor based on CNT/Graphene/TPU pyramids	Bending angle: 54.7°	4.79 MPa^{-1}	0.1 kPa - 1 MPa	-	-	[177]
2016	Pressure	CNT	Polycarbonate-urethane (PCU)	Resistive pressure sensor based on undirectional aligned CNT between elastomer layers	Strain: 500%	-	-	-	>180000 cycles	[78]
2017	Pressure	CNT	PDMS	Piezoresistance pressure sensor with interlocked microdome arrays of CNTs on elastomers	-	19.8 kPa^{-1}	0.6 - 300 Pa	Response time: 44 ms	-	[182]
2017	Pressure	CNT	PDMS	Piezoresistance pressure sensor based on CNT ink printed on PDMS	Bending angle: 22.5°	-	0-337 kPa	R^2: 0.9971	-	[81]
2017	Pressure	CNT / Au	Polyimide (PI)	Piezoresistance pressure sensor based on CNT on tissue paper	-	2.2 kPa^{-1}	35-11700 Pa	Response time: 35 ms	-	[77]
2017	Strain and Pressure	CNT	Pencil eraser	Piezoresistance pressure and strain sensor based on CNT pin-rolled on eraser	Strain: 30%	0.135 MPa^{-1}	-	R^2: 0.9803	-	[179]
2017	Pressure	CNT	TPU foam	Piezoresistance pressure sensor based on CNT/TPU foam	Strain: 77%	-	-	-	>2000 cycles	[180]
2017	Pressure	CNT / Graphene	Microstructured PDMS	Resistive pressure sensor based on sandwiched CNT/Graphene/PDMS structure	-	19.8 kPa^{-1}	0-0.3 kPa	Response time: 16.7 ms	>35000 cycles	[59]
2017	Pressure	CNT	PDMS pyramid microstructure	Piezoresistance pressure sensor based on CNT network with PDMS pyramid microstructure	Bending angle: 53.32°	8655.6 kPa^{-1}	-	Response time: 4 ms	>10000 cycles	[156]
2018	Pressure	CNT	Polyethylene naphthalate (PEN)	Piezoresistance pressure sensor based on a CNT sheet onto a micro-patterned substrate	Bending angle: 100°	7.69 kPa^{-1}	0.1-40 kPa	Detection limit: 2 Pa	>6000 cycles	[181]
2018	Pressure	PEI / CNT	Flexible fiber	Piezoresistance pressure sensor based on PEI functionalized CNT on nonconductive fibers	-	0.0025–0.052 5 MPa^{-1}	0-40 MPa	-	>550 cycles	[182]
2018	Pressure	Rubber / CNT	PDMS / epoxy	Resistive pressure sensor based on CNT thin-film transistor	Bending radius:	-	-	Response time: 30ms	-	[183]
2018	Pressure	CNT	PDMS microspheres	Piezoresistance pressure sensor based on CNT-wrapped PDMS microspheres	-	0.111 kPa^{-1}	0-50 kPa	Detection limit: 20 Pa	>10000 cycles	[157]
2018	Pressure	CNT	Polyurethane (PU)	Piezoresistance pressure sensor based on CNT/PU composite structure	-	23.35 kPa^{-1}	0-63 kPa	Hysteresis error: ±8.2%	-	[184]
2019	Pressure	CNT	Thin porous elastomer sponge	Piezoresistance pressure sensor based on CNT network-coated porous elastomer sponges	Strain: 80%	0.01–0.02 kPa^{-1}	10 Pa to 1.2 MPa	R^2: 0.98	>10000 cycles	[162]
2019	Pressure	CNT	PDMS	Piezoresistance pressure sensor based on PDMS wrapped CNT arrays	Strain: 100%	-	0-10 kPa	Response time: 26 ms	>8000 cycles	[79]
2019	Pressure	CNT	Microstructured elastomer fibers	Resistive pressure sensor based on CNT-coated elastomer fiber	-	0.17 kPa^{-1}	0-0.02 kPa	Response time: 25 ms	>10000 cycles	[185]
2019	Tactile	CNT / Carbon black NP	PDMS	Piezoresistance pressure sensor based on two CNT microstructures	Bending angle: 45°	3.2 kPa^{-1}	0-40 kPa	Response time: 217 ms	-	[186]
2019	Strain	CNT	PDMS	Piezoresistance pressure sensor based on SCA functionalized CNT/PDMS film	Strain: 350%	-	-	-	-	[187]
2020	Pressure	CNT / TPU	PI/PDMS	Piezoresistance pressure sensor based on CNT film in pyramid struture	-	41.0 MPa^{-1}	10-500 kPa	R^2: 0.99	-	[188]
2020	Pressure	CNT / Silica NP	Silicone rubber	Piezoresistance pressure sensor based on CNT/Silicone rubber composite structure	-	0.096 kPa^{-1}	0-175 kPa	-	>10000 cycles	[189]
2021	Pressure	CNT / Ag NP	PDMS	Piezoresistance pressure sensor based on Ag NPs decorated CNT film	Bending angle: 100°	0.004 kPa^{-1}	1.67-33.33 kPa	Response time: <1 s	-	[163]
2021	Pressure	CNT / PVA slurry	Polyvinylidene fluoride (PVDF) fiber network	Piezoresistance pressure sensor based on PVDF/PVA-CNTs electrospun composite film	Bending angle: 360°	0.0196 kPa^{-1}	0-40 kPa	Hysteresis: 13.1%	-	[158]
2022	Pressure	CNT	PDMS	Piezoresistance pressure sensor based on tetrahydrofuran (THF) modified CNT/PDMS	-	0.004 kPa^{-1}	0-100 kPa	Response time: 36 ms	-	[190]
2022	Pressure	CNT / PDMS	-	Piezoresistance pressure sensor based on CNT/PDMS composite porous structure	Strain: 400%	0.59 kPa^{-1}	0-260 kPa	Response time: 25 ms	>1700 cycles	[159]
2022	Pressure	CNT / Carbon fiber	PDMS	Resistive pressure sensor based on multiscale CF/CNT-PDMS composite and interdigital electrode	-	2.02 kPa^{-1}	0-185.9 kPa	Response time: 43 ms	>10000 cycles	[191]

PEDOT as a miniature mechanical sensor has been developed for *in vivo* detection of subtle physiological signals, such as respiration [143], with rapid self-healing ability, and consistent and linear responses to applied strain.

VI. CONCLUSION

This review highlights the state-of-the-art wearable and flexible CNT-based sensors that operate via electrochemical and mechanical stimuli. The development of flexible and wearable devices that can sense a variety of chemical species and mechanical behaviors is critical to advancing the healthcare industry toward real-time continuous monitoring applications. With the advent of CNTs and advancing polymer technologies, rapid advances in processing methods and innovative material combinations have correlated with their use in flexible and wearable sensors with diverse functionalities.

Sensors that do not exhibit flexibility within the industry are often fabricated with rigid metals and semiconductors, limiting their flexible capabilities. Furthermore, these methods often require multistep processes requiring various equipment that can increase expenses and process times. CNTs can be seamlessly integrated into flexible polymer materials as conductive

TABLE II
COMPARATIVE TABLE OF CNT-BASED ELECTROCHEMICAL SENSORS [12], [80], [127], [162], [169], [173], [193], [194], [195], [196], [197], [198], [199], [200], [201], [202], [203], [204], [205], [206], [207]

Publication Year	Target	Electrode Materials	Flexible Substrate	Operation Method	Flexibility	Addition Information	Durability	Reference
2014	VOC	Au NPs / CNT	Polyimide (PI)	Deposition of Au NPs on electrode for VOC sensing	Bending angle: 90°	-	>100 cycles	[192]
2015	H_2S	Cu / CNT	Polyethylene terephthalate (PET)	Cu NP decorated on electrode for H_2S gas sensing	Bending radius: >40 mm	-	>10 cycles	[193]
2015	Gas	PANI / CNT	PET	Nanocomposite networks of PANI and CNT for gas sensing	-	-	>500 cycles	[161]
2015	Biofluids	CNT	Polyurethane	Printed CNT array as electrode for biofluid sensing	Strain: 500%	-	-	[80]
2015	DNA	CNT / Au	Polydimethylsiloxane (PDMS)	CNT/polymer composite electrodes for DNA sensing	Bending angle: >90°	-	-	[12]
2016	NH_3	PANI NP / CNT	PANI fiber	Flexible PANI/CNT nanocomposite film for NH_3 sensing	Bending angle: 90°	Response time: 85 s	>800 cycles	[194]
2017	Glucose	CNT / Al foil	Polyethylene terephthalate (PET)	Dip coated GOx on CNT/ITO modified PET composite electrode	-	R^2: 0.9955	-	[195]
2017	Glucose	CNT / Pt microsphere	Carbonized silk fabric(CSF)	Immobilize GOx on CNT-coated carbonized silk fabric for glucose sensing	Bending angle: 150°	R^2: 0.991	>1000 cycles	[196]
2017	Glucose	CNT	Polyimide (PI)	Immobilize GOx on CNT based FET channel for glucose sensing	Bending angle: 90°	-	>400 cycles	[197]
2018	DNA	CNT	PDMS	CNT/PDMS composite without surface modification for DNA sensing	-	R^2: 0.9921	>7 days	[198]
2019	NO_2	PPy / N-doped CNT	Polyimide (PI)	PPy/N-doped multiwall CNTs electrode for NO_2 sensing	-	R^2: 0.9835	>1000 cycles	[199]
2019	Humidity	CNT	Flexible cellulose nanofiber	2,2,6,6-tetramethylpiperidinyl-1-oxyl (TEMPO)-oxidized NFC/CNT composite electrode for humidity sensing	Bending angle: >45°	R^2: 0.9841	-	[200]
2020	DNA	CNT	PET	Patterned VACNT on flexible PET substrate for biomarker DNA sensing	-	R^2: 0.973	>21 days	[201]
2020	Cortisol	CNT	PDMS	Poly(GMA-co-EGDMA) deposited on the CNT/PDMS as the cortisol biomimetric receptor	Strain: >100%	R^2: 0.92	>30 days	[172]
2020	Dopamine (DA)	Ni-MOF / AuNP / CNT	PDMS	Ni-MOF composite/Au NP/CNT electrodes that deposited on PDMS for DA sensing	Strain: 50%	R^2: 0.997	>4 days	[168]
2020	Glucose	CNT/Au	Paper	CNT-coated paper-based electrodes for glucose sensing	Bending angle: >360°	-	-	[202]
2021	Electrochemical	CNT	Cellulose-based flexible film	A conductive polymer with NW film and CNTs for electrochemcial sensing.	Strain: <10%	-	-	[203]
2021	HIV DNA	Ni / Au NP / CNT	Polyvinyl alcohol(PVA)	Ni-MOF composite/AuNPs/CNTs film electrode for HIV DNA sensing	Strain: 20%	R^2: 0.995	>20 days	[127]
2021	H_2O_2	Nano-Au / CNT	PDMS	Network of nano-Au/CNT electrodes in PDMS for H_2O_2 sensing	Strain: 50%	-	>100 cycles	[204]
2021	H_2O_2	Prussian Blue / CNT	PDMS	PDMS membrane supported PB@CNT array for H_2O_2 sensing	-	-	>100 cycles	[205]
2021	Nitrite	LIG / Au NP / CNT	Polyimide (PI)	Laser-induced graphene (LIG)/CNT/Au NPs electrode for Nitirte sensing	-	R^2: 0.996	-	[206]

materials for electrode designs. Furthermore, their inherent mechanical properties and favorable size allow them to be easily incorporated into common flexible substrate synthesis methods, including dip coating, inkjet printing drop-casting, and direct polymerization. In addition to these favorable fabrication enabling properties, CNTs as individual components also have high flexibility, electrochemical stability, and desirable electronic properties, making them ideal candidates for flexible sensors.

While CNTs can enhance the strain range of flexible sensors due to their excellent mechanical properties [154], the antistrain property of aligned CNT-based sensors strongly depends on the deformation direction [155]; while, for electrochemical sensing, the chemical concentration is measured through the change of an electrical signal, its change is composed of two parts: 1) sensing target and 2) strain deformation, in measuring deformation. This problem could be overcome, to some extent, by incorporating CNT-flexible substrate composites in specific architectures to modify the mechanical properties of devices for different applications, such as pyramid microstructure [156], microspheres [157], and micropillar array patterns [98].

Tables I and II summarize the progress in developing flexible and wearable sensors based on CNTs in terms of mechanisms, material, and several aspects of performance for mechanical and electrochemical sensors, respectively. For comparison, flexible mechanical and electrochemical sensors that do not contain CNTs are shown in Tables III and IV. Flexible sensors can be divided into two categories: flexible mechanical sensors and flexible electrochemical sensors.

TABLE III
COMPARATIVE TABLE OF NON-CNT-BASED MECHANICAL SENSORS [4], [165], [166], [167], [208], [209], [210], [211], [212], [213], [214], [215], [216], [217], [218], [219], [220], [221], [222], [223], [224]

Publication Year	Target	Electrode Materials	Flexible Substrate	Operation Method	Flexibility	Sensitivity	Sensing Range	Addition Information	Durability	Reference
2004	Pressure	Graphite particles	PDMS	Piezoresistance pressure sensor based on organic transistors integrated with a graphite-containing rubber layer	Strain: 1.5%	-	0-30 kPa	-	-	[207]
2015	Pressure	Silver nanowires	PDMS	Resistive pressure sensor based on silver NWs/PDMS elastomeric electrode	-	>3.8 kPa^{-1}	-	Response time: 150 ms	-	[208]
2016	Pressure	Au	PDMS	Piezoresistance pressure sensor based on gold electrode on porous PDMS	Bending angle: >45°	1.18 kPa^{-1}	0.02 kPa	Response time: 150 ms	-	[222]
2017	Pressure	GO	Polyester fabric	Resistive pressure sensor based on 3D multi-layer structure graphene textile	-	0.0017 kPa^{-1}	0-230 kPa	-	>120 cycles	[210]
2017	Pressure	Silver nanowires	PDMS	Resistive pressure sensor based on silver nanowires/PDMS microarray structure	Bending angle: >180°	2.94 kPa^{-1}	0-6.7 kPa	Pressure detection limit: 3 Pa	>1000 cycles	[211]
2017	Pressure	CU nanowires	Porous foam	Piezoresistance pressure sensor based on Cu NW areogel	Strain: <60%	0.02-0.7 kPa^{-1}	-	Response time: 80 ms	>200 cycles	[164]
2017	Pressure	rGO / TNL	Polyvinylidene fluoride (PVDF)	Piezoresistance pressure sensor based on PVDF/rGO-TNL composite	Strain: 4%	-	0-17.6 kPa	Response time: 10 ms	-	[212]
2018	pressure	PDMS / Ag NWs and PET / ITO	PVDF nanofiber film	Piezoresistance pressure sensor based on electrospinning-prepared PVDF nanofiber film	Strain: 320%	-	-	-	>1000 cycles	[213]
2018	Pressure	rGO	PANI NWs	Piezoresistance pressure sensor based on rGO/polyaniline wrapped sponge	-	0.042-0.152 kPa^{-1}	0–27 kPa	Response time: 96 ms	9000 cycles	[4]
2018	Pressure	Graphene	PDMS	Piezoresistance pressure sensor based on micropatterned graphene/PDMS	Bending angle: <90°	0.0078-0.24 kPa^{-1}	0-100 kPa	Response time: 65 ms	>2000 cycles	[165]
2018	Pressure	Graphene ink	Lotus leaf	Piezoresistive pressure sensor based on arrays of microscale papillae	-	1.2 kPa^{-1}	0-25 kPa	-	-	[214]
2018	Pressure	rGO/polystyrene ball core–shell	PDMS	Resistive pressure sensor based on sandwiching a core–shell film layer between two thin flexible PDMS sheets	-	50.9 kPa^{-1}	3–1000 Pa	Pressure detection limit: 3 Pa	>20000 cycles	[215]
2019	Pressure	Metal electrode	MXene–textile / PI	Piezoresistive pressure sensor based on MXene–textile prepared via dip-coating	-	3.844 kPa^{-1}	0-29 kPa	Response time: 26 ms	5600 cycles	[216]
2019	Pressure	Pt NPs	Polypyrrole / PDMS	Piezoresistance pressure sensor based on saw-toothed electrodes	Bending angle: >180°	0.003-0.722 kPa^{-1}	0-20 kPa	Response time: 60 ms	-	[166]
2020	Pressure	rGO	Flexible wood (FW)	Piezoresistance pressure sensor based on rGO-modified flexible wood	Bending angle: >360°	1.85 kPa^{-1}	0-60 kPa	-	>10000 cycles	[217]
2020	Pressure	Ti / Au	PDMS pyramid arrays	Piezoresistance pressure sensor based on sandwiched electrodes	Strain: <55%	70.6 kPa^{-1}	-	Pressure detection limit: 1 Pa	>10200 cycles	[218]
2020	Pressure	TiO_2 nanofibers	PI	Resistive pressure sensor based on Ceramic nanofibers	Strain: <60%	4.4 kPa^{-1}	-	Pressure detection limit: 0.8 Pa	>50000 cycles	[219]
2020	Pressure	Ag thin-film	PDMS	Piezoresistance pressure sensor based on two opposing elastomers coated with high conductive materials	Strain: 27%	5.9 kPa^{-1}	0-15 kPa	Response time: 53 ms	>500 cycles	[220]
2021	Pressure	Carbon NPs / CFs	PDMS	Piezoresistance pressure sensor based on CFs/CNPs/PDMS conductive network	-	26.6kPa^{-1}	20 Pa-600 kPa	-	>5000 cycles	[221]
2021	Pressure	Polyester tape	Paper	Resistive pressure sensor based on rough paper and polyester conductive tape	Bending angle: >360°	0.23 kPa^{-1}	0.1-2 kPa	Response time: 41 ms	>5000 cycles	[222]
2022	Pressure	Rough PU / Ag	PU nanofibers film	Piezoresistance pressure sensor based on electrospun rough PU nanofibers film	Bending angle: 360°	0.97-10.53 kPa^{-1}	0-15 kPa	Response time: 60 ms	>10000 cycles	[223]

Compared to pressure sensors without CNTs, the CNT-based sensors show a wide sensing range [158] and rapid (e.g., 25 ms) response time [159], provided by an efficient electron transfer [160]. Furthermore, CNTs can enhance the strain range of flexible sensors due to their mechanical properties [161], resulting in 400% tensile or compression strain [159]. On the other hand, the sensitivity of the CNT-based sensors often demonstrates smaller variations than those based on other materials [162], [163], [164], [165], [166]. For electrochemical sensing, CNT-based sensors show better stretchability and less bendability than other sensors based on other materials [156]. However, the flexibility of aligned CNT-based sensors strongly depends on the deformation direction [155]. Also, CNTs show higher stretchability than bendability [167]; when an external load is applied along the perpendicular direction of the CNT sheet, the CNTs tend to produce cracks to form a rough fracture surface, changing their electrical properties under bending conditions. As for durability, CNT-based flexible electrochemical sensors have shorter working life [127], [168], [169], [170], [171]. However, combining CNTs with other materials as a protection layer can prolong the working life, such as the imprinted (MIP) poly(GMA-co-EGDMA) deposited on the CNTs, which can realize 30 days of working life [172].

For future consideration, developmental research of stretchable and flexible sensors containing CNTs must continue to be expanded in diverse arrangements, functionalities, and material combinations to widen the field's potential applications and performances. Further research must be pursued in taking advantage of CNTs toward tailoring their function and specification in combination with multimodal sensing and single devices that can sense a multitude of chemical species and/or mechanical disturbances simultaneously via microelectrode arrays. Future developments need to be pursued in combining these flexible sensors into compact independent devices that include energy storage and data storage and/or transmission within a single device that could be used on the human body. Additional methods enabling high sensing performance while

TABLE IV
COMPARATIVE TABLE OF NON-CNT-BASED MECHANICAL SENSORS [170], [171], [172], [225], [226], [227], [228], [229], [230], [231], [232], [233], [234], [235], [236], [237], [238], [239], [240], [241], [242], [243], [244]

Publicaitio n Year	Target	Electrode Materials	Flexible Substrate	Operation Method	Flexibility	Addition Information	Durability	Reference
2017	NADH	Graphite	Paper	Direct drawing method of graphite onto paper for NADH sensing	-	-	-	[224]
2017	4−aminophenol (AP) and 4−chlorophenol (CP)	Graphene oxide / Pt	Wrapped hierarchical hollow structured SnO_2 spheres	Graphene oxide−wrapped SnO_2 hollow spheres for 4−AP and 4−CP sensing	-	-	-	[225]
2017	Electrochemical	Carbon black	Paper	Fully-printed carbon black nanostructures on paper for electrochemical sensing	Bending angle: >180°	-	>20000 cycles	[226]
2018	Glucose	Guanosine and KB(OH)4	Polyaniline (PANI)	Self-assembled enzyme-like nanofibrous G-Molecular hydrogel for glucose sensing	-	-	>100 cycles	[227]
2018	Uric acid	MoS_2	Aluminium foil (Al)	Hydrothermally grown MoS_2 on aluminium foil for uric acid sensing	-	R^2: 0.999	>150 cycles	[228]
2018	pH value	CuO	Poly(ethylene terephthalate) (PET)	CuO nanostructures with NR morphology flexible substrate for pH sensing	Bending angle: >33°	-	-	[229]
2018	PpHH value	Carbon ink / Ag ink	PET	Conductive ink is printed on flexible substrate for pH sensing	-	-	-	[230]
2019	H_2O_2	Graphene / Ag NPs	PET	Laser scribed Graphene/Ag NPs on flexible substrate for H_2O_2 sensing	Bending radius: >5 mm	R^2: 0.9982	>80 cycles	[231]
2019	Hydroquinone (HQ)	Nail polish and graphite	PET	Conductive ink is prepared with nail polish and graphite on PET for HQ sensing	Bending angle: <180°	-	-	[232]
2019	Calcium and chloride ions	Ag NWs	PDMS	AgNW/PDMS composite structure for calcium and chloride ions sensing	Strain: <50%	R^2: 0.99997	-	[233]
2019	Glucose	CuO / NiO-C	Cello tape (CT)	Hierarchical CuO/NiO-Carbon derived from MOF on CT for glucose sensing	Bending angle: >180°	-	>56 days	[169]
2019	Glucose	Gold/MoS_2/gold nanofilm	Polymer substrate	Immobilizing GOx on flexible polymer with Au/MoS_2 for glucose sensing	Flexure strength: 11.2 MPa	-	-	[234]
2019	Dopamine (DA)	Pt-AuNPs / LIG	Polyimide (PI)	Pt-Au NP-modified LIG on flexible substrate for DA sensing	Strain: <20%	R^2: 0.9956	-	[235]
2020	Nitric oxide (NO)	Au	Copolymer of PLLA–PTMC	Biocompatible poly(eugenol) film as selective membrane for NO Sensing	-	Response time: 350 ms	>7 days	[236]
2020	DA	Carbon ink	PET	Carbon ink based screen-printed carbon electrodes for DA sensing	Bending angle: <180°	R^2: 0.985	-	[237]
2020	Parkinson's disease biomarkers	Pt	Bio-PET	Antibody functionalized electrode for Parkinson's disease protein sensing	-	R^2: 0.98	>4 times	[238]
2020	Uric acid	Au NPs	N-doped BSA carbon matrix	AuNP@NBSAC-modified three-electrode for uric acid sensing	-	R^2: 0.9984	>30 days	[239]
2021	DA	PPy(PEE)	PPy doped with 2-naphthalene	Sanwiched Modified PPy films for DA sensing	Strain: 41.6%	R^2: 0.9987	>1000 cycles	[240]
2021	Pb^{2+} ions	Cu-chitosan	Polyvinyl chloride (PVC) film	Screen-printed Cu-chitosan on flexible substrate for heavy metal ions sensing	Bending angle: >180°	R^2: 0.9935	-	[241]
2021	DA	ZnS NPs-decorated	Paper	ZnS NPs decorated composite graphene paper electrode (CGPE) for DA sensing	Bending angle: >180°	R^2: 0.9973	>30 days	[170]
2022	Lactate	Screen-printed electrode	PEDOT	PEDOT was transferred to a flexible screen-printed electrode for lactate sensing	Bending angle: >135°	R^2: 0.993	>30 days	[171]
2022	Chloramphenicol (CAP), clenbuterol (CLB) and ractopamine (RAC)	Flexible graphene electrodes	Nitrile gloves	Laser-enabled graphene electrode on flexible gloves for fast food security detection	Bending radius: <4.5 cm	R^2: 0.992-0.995	-	[242]
2022	Heavy metal ions	Bi NP @ LIG	Nafion	Nafion was pipetted on BiNP@LIG for heavy metal ions sensing	-	R^2: 0.98-0.992	-	[243]

shielding the sensor from its environment need to be further developed, considering the long-term use of flexible sensors in practical wearable applications. Long-term use also needs to be explored in more detail, including incorporating and studying passivation layers to protect the wearable sensor and allow breathability for adequate gas exchange and perspiration. Owing to their properties and diverse applications demonstrated in the literature, CNTs are prime candidate materials for flexible electrode designs for developing next-generation wearable sensors for wearable electronics and healthcare applications.

REFERENCES

[1] D. R. Seshadri, J. R. Rowbottom, C. Drummond, J. E. Voos, and J. Craker, "A review of wearable technology: Moving beyond the hype: From need through sensor implementation," in *Proc. 8th Cairo Int. Biomed. Eng. Conf. (CIBEC)*, Dec. 2016, pp. 52–55.

[2] C. Zhang *et al.*, "Fluid-driven artificial muscles: Bio-design, manufacturing, sensing, control, and applications," *Bio-Des. Manuf.*, vol. 4, no. 1, pp. 123–145, Mar. 2021.

[3] T. Huynh and H. Haick, "Autonomous flexible sensors for health monitoring," *Adv. Mater.*, vol. 30, no. 50, Dec. 2018, Art. no. 1802337.

[4] G. Ge *et al.*, "A flexible pressure sensor based on rGO/polyaniline wrapped sponge with tunable sensitivity for human motion detection," *Nanoscale*, vol. 10, no. 21, pp. 10033–10040, 2018, doi: 10.1039/C8NR02813C.

[5] Y. Huang, D. Fang, C. Wu, W. Wang, X. Guo, and P. Liu, "A flexible touch-pressure sensor array with wireless transmission system for robotic skin," *Rev. Sci. Instrum.*, vol. 87, no. 6, Jun. 2016, Art. no. 065007.

[6] Q. Shi, Z. Zhang, T. Chen, and C. Lee, "Minimalist and multifunctional human machine interface (HMI) using a flexible wearable triboelectric patch," *Nano Energy*, vol. 62, pp. 355–366, Aug. 2019.

[7] A. Nag, S. C. Mukhopadhyay, and J. Kosel, "Wearable flexible sensors: A review," *IEEE Sensors J.*, vol. 17, no. 3, pp. 3949–3960, Jul. 2017.

[8] A. P. Graham *et al.*, "Towards the integration of carbon nanotubes in microelectronics," *Diamond Rel. Mater.*, vol. 13, nos. 4–8, pp. 1296–1300, Apr. 2004.

[9] M. Arefin, "Empirical equation based chirality (n, m) assignment of semiconducting single wall carbon nanotubes from resonant Raman scattering data," *Nanomaterials*, vol. 3, no. 1, pp. 1–21, Dec. 2012, doi: 10.3390/nano3010001.

[10] S. Kumar *et al.*, "Review—Recent advances in the development of carbon nanotubes based flexible sensors," *J. Electrochem. Soc.*, vol. 167, no. 4, Feb. 2020, Art. no. 047506.

[11] J. Bae *et al.*, "Study on the sensing signal profiles for determination of process window of flexible sensors based on surface treated PDMS/CNT composite patches," *Polymers*, vol. 10, no. 9, p. 951, Aug. 2018.

[12] J. Li and E.-C. Lee, "Carbon nanotube/polymer composite electrodes for flexible, attachable electrochemical DNA sensors," *Biosensors Bioelectron.*, vol. 71, pp. 414–419, Sep. 2015, doi: 10.1016/j.bios.2015.04.045.

[13] E. Bakker and M. Telting-Diaz, "Electrochemical sensors," *Anal. Chem.*, vol. 74, no. 12, pp. 2781–2800, 2002.

[14] J. Li, A. Cassell, L. Delzeit, J. Han, and M. Meyyappan, "Novel three-dimensional electrodes: Electrochemical properties of carbon nanotube ensembles," *J. Phys. Chem. B*, vol. 106, no. 36, pp. 9299–9305, Sep. 2002, doi: 10.1021/jp021201n.

[15] B.-R. Adhikari, M. Govindhan, and A. Chen, "Carbon nanomaterials based electrochemical sensors/biosensors for the sensitive detection of pharmaceutical and biological compounds," *Sensors*, vol. 15, no. 9, pp. 22490–22508, Sep. 2015, doi: 10.3390/s150922490.

[16] Z. Çelik-Butler and D. P. Butler, "Flexible sensors—A review," *J. Nanoelectron. Optoelectron.*, vol. 1, no. 2, pp. 194–202, 2006.

[17] M. Lowe, A. King, E. Lovett, and T. Papakostas, "Flexible tactile sensor technology: Bringing haptics to life," *Sensor Rev.*, vol. 24, no. 1, pp. 33–36, Mar. 2004.

[18] J.-K. Lee, S.-S. Kim, Y.-I. Park, C.-D. Kim, and Y.-K. Hwang, "In-cell adaptive touch technology for a flexible e-paper display," *Solid-State Electron.*, vol. 56, no. 1, pp. 159–162, Feb. 2011.

[19] R. Rahimi *et al.*, "A low-cost flexible pH sensor array for wound assessment," *Sens. Actuators B, Chem.*, vol. 229, pp. 609–617, Jun. 2016.

[20] M. Amjadi, K. U. Kyung, I. Park, and M. Sitti, "Stretchable, skin-mountable, and wearable strain sensors and their potential applications: A review," *Adv. Funct. Mater.*, vol. 26, no. 11, pp. 1678–1698, 2016.

[21] H.-K. Lee, S.-I. Chang, and E. Yoon, "A flexible polymer tactile sensor: Fabrication and modular expandability for large area deployment," *Microelectromech. Syst., J.*, vol. 15, no. 6, pp. 1681–1686, Dec. 2006.

[22] S. Rana, P. Subramani, R. Fangueiro, and A. G. Correia, "A review on smart self-sensing composite materials for civil engineering applications," *AIMS Mater. Sci.*, vol. 3, no. 2, pp. 357–379, 2016.

[23] P. Hu, H. Wang, G. Tian, Y. Liu, X. Li, and B. F. Spencer, "Multifunctional flexible sensor array-based damage monitoring for switch rail using passive and active sensing," *Smart Mater. Struct.*, vol. 29, no. 9, Sep. 2020, Art. no. 095013.

[24] O. Kanoun, A. Bouhamed, R. Ramalingame, J. R. Bautista-Quijano, D. Rajendran, and A. Al-Hamry, "Review on conductive polymer/CNTs nanocomposites based flexible and stretchable strain and pressure sensors," *Sensors*, vol. 21, no. 2, p. 341, Jan. 2021.

[25] S. Park, M. Vosguerichian, and Z. Bao, "A review of fabrication and applications of carbon nanotube film-based flexible electronics," *Nanoscale*, vol. 5, no. 5, pp. 1727–1752, Mar. 2013.

[26] M. Eguílaz *et al.*, "Recent advances in the development of electrochemical hydrogen peroxide carbon nanotube-based (bio)sensors," *Current Opinion Electrochem.*, vol. 14, pp. 157–165, Apr. 2019.

[27] T. Yan, Y. Wu, W. Yi, and Z. Pan, "Recent progress on fabrication of carbon nanotube-based flexible conductive networks for resistive-type strain sensors," *Sens. Actuators A, Phys.*, vol. 327, Aug. 2021, Art. no. 112755.

[28] S. Iijima, "Helical microtubules of graphitic carbon," *Nature*, vol. 354, no. 6348, p. 56, 1991.

[29] C. Rüchardt and H.-D. Beckhaus, "Towards an understanding of the carbon-carbon bond," *Angew. Chem. Int. Ed. English*, vol. 19, no. 6, pp. 429–440, Jun. 1980.

[30] D. Tasis, N. Tagmatarchis, A. Bianco, and M. Prato, "Chemistry of carbon nanotubes," *Chem. Rev.*, vol. 106, no. 3, pp. 1105–1136, 2006.

[31] S. Huang, C. Zhao, W. Pan, Y. Cui, and H. Wu, "Direct writing of half-meter long CNT based fiber for flexible electronics," *Nano Lett.*, vol. 15, no. 3, pp. 1609–1614, Mar. 2015.

[32] B. Q. Wei, R. Vajtai, and P. M. Ajayan, "Reliability and current carrying capacity of carbon nanotubes," *Appl. Phys. Lett.*, vol. 79, no. 8, pp. 1172–1174, Aug. 2001.

[33] M. M. Shokrieh and R. Rafiee, "A review of the mechanical properties of isolated carbon nanotubes and carbon nanotube composites," *Mech. Compos. Mater.*, vol. 46, no. 2, pp. 155–172, Jul. 2010.

[34] J. H. Jung, G. B. Hwang, J. E. Lee, and G. N. Bae, "Preparation of airborne Ag/CNT hybrid nanoparticles using an aerosol process and their application to antimicrobial air filtration," *Langmuir*, vol. 27, no. 16, pp. 10256–10264, Aug. 2011.

[35] T. Zhang, S. Mubeen, N. V. Myung, and M. A. Deshusses, "Recent progress in carbon nanotube-based gas sensors," *Nanotechnology*, vol. 19, no. 33, Aug. 2008, Art. no. 332001, doi: 10.1088/0957-4484/19/33/332001.

[36] R. Zhang, A. Palumbo, J. Xu, and E. H. Yang, "CNT-based stretchable supercapacitors," in *Nanoengineering, Quantum Sciences, and Nanotechnology Handbook*. Boca Raton, FL, USA: CRC Press, 2019.

[37] L.-M. Peng, Z. Zhang, and S. Wang, "Carbon nanotube electronics: Recent advances," *Mater. Today*, vol. 17, no. 9, pp. 433–442, Nov. 2014.

[38] S. M. Andersen *et al.*, "Durability of carbon nanofiber (CNF) & carbon nanotube (CNT) as catalyst support for proton exchange membrane fuel cells," *Solid State Ionics*, vol. 231, pp. 94–101, Feb. 2013.

[39] Y. Cheng and O. Zhou, "Electron field emission from carbon nanotubes," *Comp. Rendus Phys.*, vol. 4, no. 9, pp. 1021–1033, Nov. 2003.

[40] M. S. Dresselhaus, G. Dresselhaus, and A. Jorio, "Unusual properties and structure of carbon nanotubes," *Annu. Rev. Mater. Res.*, vol. 34, no. 1, pp. 247–278, Aug. 2004.

[41] M. Tambraparni and S. Wang, "Separation of metallic and semiconducting carbon nanotubes," *Recent Patents Nanotechnol.*, vol. 4, no. 1, pp. 1–9, Jan. 2010.

[42] S. Jabeen, A. Kausar, B. Muhammad, S. Gul, and M. Farooq, "A review on polymeric nanocomposites of nanodiamond, carbon nanotube, and nanobifiller: Structure, preparation and properties," *Polym., Plastics Technol. Eng.*, vol. 54, no. 13, pp. 1379–1409, Sep. 2015, doi: 10.1080/03602559.2015.1021489.

[43] D. M. Gattia, M. V. Antisari, R. Marazzi, L. Pilloni, V. Contini, and A. Montone, "Arc-discharge synthesis of carbon nanohorns and multiwalled carbon nanotubes," *Mater. Sci. Forum*, vol. 518, pp. 23–28, Jul. 2006, doi: 10.4028/www.scientific.net/MSF.518.23.

[44] Z. Shi *et al.*, "Mass-production of single-wall carbon nanotubes by arc discharge method," *Carbon*, vol. 37, no. 9, pp. 1449–1453, 1999, doi: 10.1016/S0008-6223(99)00007-X.

[45] H. Dai, "Nanotube growth and characterization," in *Carbon Nanotubes*. Berlin, Germany: Springer, 2001, pp. 29–53.

[46] S.-L. Chou, Y. Zhao, J.-Z. Wang, Z.-X. Chen, H.-K. Liu, and S.-X. Dou, "Silicon/single-walled carbon nanotube composite paper as a flexible anode material for lithium ion batteries," *J. Phys. Chem. C*, vol. 114, no. 37, pp. 15862–15867, Sep. 2010, doi: 10.1021/jp1063403.

[47] M. Su, B. Zheng, and J. Liu, "A scalable CVD method for the synthesis of single-walled carbon nanotubes with high catalyst productivity," *Chem. Phys. Lett.*, vol. 322, no. 5, pp. 321–326, 2000, doi: 10.1016/S0009-2614(00)00422-X.

[48] A. Szabó *et al.*, "Influence of synthesis parameters on CCVD growth of vertically aligned carbon nanotubes over aluminum substrate," *Sci. Rep.*, vol. 7, no. 1, p. 9557, Dec. 2017.

[49] C. J. Lee, J. Park, and J. A. Yu, "Catalyst effect on carbon nanotubes synthesized by thermal chemical vapor deposition," *Chem. Phys. Lett.*, vol. 360, nos. 3–4, pp. 250–255, Jul. 2002.

[50] M. Chhowalla *et al.*, "Growth process conditions of vertically aligned carbon nanotubes using plasma enhanced chemical vapor deposition," *J. Appl. Phys.*, vol. 90, no. 10, pp. 5308–5317, Nov. 2001, doi: 10.1063/1.1410322.

[51] G. Hong, Y. Chen, P. Li, and J. Zhang, "Controlling the growth of single-walled carbon nanotubes on surfaces using metal and non-metal catalysts," *Carbon*, vol. 50, no. 6, pp. 2067–2082, May 2012.

[52] C. Hu and S. Hu, "Carbon nanotube-based electrochemical sensors: Principles and applications in biomedical systems," *J. Sensors*, vol. 2009, pp. 1–40, Nov. 2009, doi: 10.1155/2009/187615.

[53] R. Zhang *et al.*, "A flexible pressure sensor with sandwiched carpets of vertically aligned carbon nanotubes partially embedded in polydimethylsiloxane substrates," *IEEE Sensors J.*, vol. 20, no. 20, pp. 12146–12153, Oct. 2020, doi: 10.1109/JSEN.2020.2999261.

[54] R. Zhang, K. Yan, A. Palumbo, J. Xu, S. Fu, and E.-H. Yang, "A stretchable and bendable all-solid-state pseudocapacitor with dodecylbenzenesulfonate-doped polypyrrole-coated vertically aligned carbon nanotubes partially embedded in PDMS," *Nanotechnology*, vol. 30, no. 9, Mar. 2019, Art. no. 095401.

[55] R. Zhang, J. Ding, and E. H. Yang, "Highly stretchable supercapacitors enabled by interwoven CNTs partially embedded in PDMS," *ACS Appl. Energy Mater.*, vol. 1, no. 5, pp. 2048–2055, 2018, doi: 10.1021/acsaem.8b00156.

[56] J. Ding *et al.*, "Graphene—Vertically aligned carbon nanotube hybrid on PDMS as stretchable electrodes," *Nanotechnology*, vol. 28, no. 46, Nov. 2017, Art. no. 465302.

[57] T. Y. Tsai, C. Y. Lee, N. H. Tai, and W. H. Tuan, "Transfer of patterned vertically aligned carbon nanotubes onto plastic substrates for flexible electronics and field emission devices," *Appl. Phys. Lett.*, vol. 95, no. 1, Jul. 2009, Art. no. 013107.

[58] Y. Zhang *et al.*, "Tailoring the morphology of carbon nanotube arrays: From spinnable forests to undulating foams," *ACS Nano*, vol. 3, no. 8, pp. 2157–2162, Aug. 2009.

[59] M. Jian *et al.*, "Flexible and highly sensitive pressure sensors based on bionic hierarchical structures," *Adv. Funct. Mater.*, vol. 27, no. 9, Mar. 2017, Art. no. 1606066, doi: 10.1002/adfm.201606066.

[60] M. B. Jakubinek *et al.*, "Thermal and electrical conductivity of tall, vertically aligned carbon nanotube arrays," *Carbon*, vol. 48, no. 13, pp. 3947–3952, 2010.

[61] J. Li *et al.*, "Electronic properties of multiwalled carbon nanotubes in an embedded vertical array," *Appl. Phys. Lett.*, vol. 81, no. 5, pp. 910–912, Jul. 2002.

[62] T. Saito, K. Matsushige, and K. Tanaka, "Chemical treatment and modification of multi-walled carbon nanotubes," *Phys. B, Condens. Matter*, vol. 323, nos. 1–4, pp. 280–283, Oct. 2002.

[63] C. A. Furtado, U. J. Kim, H. R. Gutierrez, L. Pan, E. C. Dickey, and P. C. Eklund, "Debundling and dissolution of single-walled carbon nanotubes in amide solvents," *J. Amer. Chem. Soc.*, vol. 126, no. 19, pp. 6095–6105, May 2004, doi: 10.1021/ja039588a.

[64] G. Fortier, M. Vaillancourt, and D. Bélanger, "Evaluation of Nafion as media for glucose oxidase immobilization for the development of an amperometric glucose biosensor," *Electroanalysis*, vol. 4, no. 3, pp. 275–283, Mar. 1992, doi: 10.1002/elan.1140040304.

[65] C. Cai and J. Chen, "Direct electron transfer of glucose oxidase promoted by carbon nanotubes," *Anal. Biochem.*, vol. 332, no. 1, pp. 75–83, Sep. 2004, doi: 10.1016/j.ab.2004.05.057.

[66] M. Zhang, A. Smith, and W. Gorski, "Carbon nanotube–chitosan system for electrochemical sensing based on dehydrogenase enzymes," *Anal. Chem.*, vol. 76, no. 17, pp. 5045–5050, Sep. 2004, doi: 10.1021/ac049519u.

[67] Y. Liu *et al.*, "Polyethylenimine-grafted multiwalled carbon nanotubes for secure noncovalent immobilization and efficient delivery of DNA," *Angew. Chem. Int. Ed.*, vol. 44, no. 30, pp. 4782–4785, Jul. 2005, doi: 10.1002/anie.200500042.

[68] V. G. Gavalas, S. A. Law, J. C. Ball, R. Andrews, and L. G. Bachas, "Carbon nanotube aqueous sol-gel composites: Enzyme-friendly platforms for the development of stable biosensors," *Anal. Biochem.*, vol. 329, no. 2, pp. 247–252, Jun. 2004, doi: 10.1016/j.ab.2004.02.025.

[69] A. A. Mamedov, N. A. Kotov, M. Prato, D. M. Guldi, J. P. Wicksted, and A. Hirsch, "Molecular design of strong single-wall carbon nanotube/polyelectrolyte multilayer composites," *Nature Mater.*, vol. 1, no. 3, pp. 190–194, Nov. 2002, doi: 10.1038/nmat747.

[70] Z. Liu *et al.*, "Organizing single-walled carbon nanotubes on gold using a wet chemical self-assembling technique," *Langmuir*, vol. 16, no. 8, pp. 3569–3573, Apr. 2000, doi: 10.1021/la9914110.

[71] D. Zheng, C. Hu, Y. Peng, W. Yue, and S. Hu, "Noncovalently functionalized water-soluble multiwall-nanotubes through azocarmine B and their application in nitric oxide sensor," *Electrochem. Commun.*, vol. 10, no. 1, pp. 90–94, Jan. 2008, doi: 10.1016/j.elecom.2007.10.027.

[72] A. Bouhamed, A. Al-Hamry, C. Müller, S. Choura, and O. Kanoun, "Assessing the electrical behaviour of MWCNTs/epoxy nanocomposite for strain sensing," *Compos. B, Eng.*, vol. 128, pp. 91–99, Nov. 2017, doi: 10.1016/j.compositesb.2017.07.005.

[73] Q.-H. Zhang and D.-J. Chen, "Percolation threshold and morphology of composites of conducting carbon black/polypropylene/EVA," *J. Mater. Sci.*, vol. 39, no. 5, pp. 1751–1757, Mar. 2004, doi: 10.1023/B:JMSC.0000016180.42896.0f.

[74] N. T. Dinh and O. Kanoun, "Temperature-compensated force/pressure sensor based on multi-walled carbon nanotube epoxy composites," *Sensors*, vol. 15, no. 5, pp. 11133–11150, 2015, doi: 10.3390/s150511133.

[75] J. R. Bautista-Quijano, R. Torres, and O. Kanoun, "Flexible strain sensing filaments based on styrene-butadiene-styrene co-polymer mixed with carbon particle filled thermoplastic polyurethane," in *Proc. Nanotechnol. Instrum. Meas. (NANOfIM)*, Nov. 2018, pp. 7–9, doi: 10.1109/NANOFIM.2018.8688618.

[76] H.-M. So, J. W. Sim, J. Kwon, J. Yun, S. Baik, and W. S. Chang, "Carbon nanotube based pressure sensor for flexible electronics," *Mater. Res. Bull.*, vol. 48, no. 12, pp. 5036–5039, 2013, doi: 10.1016/j.materresbull.2013.07.022.

[77] Z. Zhan *et al.*, "Paper/carbon nanotube-based wearable pressure sensor for physiological signal acquisition and soft robotic skin," *ACS Appl. Mater. Interfaces*, vol. 9, no. 43, pp. 37921–37928, Nov. 2017, doi: 10.1021/acsami.7b10820.

[78] J. Park *et al.*, "Giant tunneling piezoresistance of composite elastomers with interlocked microdome arrays for ultrasensitive and multimodal electronic skins," *ACS Nano*, vol. 8, no. 5, pp. 4689–4697, May 2014, doi: 10.1021/nn500441k.

[79] Z. Zhang *et al.*, "Simple and efficient pressure sensor based on PDMS wrapped CNT arrays," *Carbon*, vol. 155, pp. 71–76, Dec. 2019, doi: 10.1016/j.carbon.2019.08.018.

[80] A. J. Bandodkar, I. Jeerapan, J.-M. You, R. Nuñez-Flores, and J. Wang, "Highly stretchable fully-printed CNT-based electrochemical sensors and biofuel cells: Combining intrinsic and design-induced stretchability," *Nano Lett.*, vol. 16, no. 1, pp. 721–727, Jan. 2016, doi: 10.1021/acs.nanolett.5b04549.

[81] D. Maddipatla, B. B. Narakathu, M. M. Ali, A. A. Chlaihawi, and M. Z. Atashbar, "Development of a novel carbon nanotube based printed and flexible pressure sensor," in *Proc. IEEE Sensors Appl. Symp. (SAS)*, Apr. 2017, pp. 1–4, doi: 10.1109/SAS.2017.7894034.

[82] M. B. Jakubinek *et al.*, "Single-walled carbon nanotube–epoxy composites for structural and conductive aerospace adhesives," *Compos. B, Eng.*, vol. 69, pp. 87–93, Feb. 2015, doi: 10.1016/j.compositesb.2014.09.022.

[83] Y. J. Jung *et al.*, "Aligned carbon nanotube–polymer hybrid architectures for diverse flexible electronic applications," *Nano Lett.*, vol. 6, no. 3, pp. 413–418, Mar. 2006, doi: 10.1021/nl052238x.

[84] A. I. Oliva-Avilés, F. Avilés, and V. Sosa, "Electrical and piezoresistive properties of multi-walled carbon nanotube/polymer composite films aligned by an electric field," *Carbon*, vol. 49, no. 9, pp. 2989–2997, Aug. 2011, doi: 10.1016/j.carbon.2011.03.017.

[85] S.-J. Woo, J.-H. Kong, D.-G. Kim, and J.-M. Kim, "A thin all-elastomeric capacitive pressure sensor array based on micro-contact printed elastic conductors," *J. Mater. Chem. C*, vol. 2, no. 22, pp. 4415–4422, 2014, doi: 10.1039/x0xx00000x.

[86] R. Zhang, K. Yan, A. Palumbo, J. Xu, S. Fu, and E.-H. Yang, "A stretchable and bendable all-solid-state pseudocapacitor with dodecylbenzenesulfonate-doped polypyrrole-coated vertically aligned carbon nanotubes partially embedded in PDMS," *Nanotechnology*, vol. 30, no. 9, Mar. 2019, Art. no. 095401, doi: 10.1088/1361-6528/aaf135.

[87] R. Zhang and E. H. Yang, "Flexible supercapacitors consisting of vertically aligned carbon nanotubes on PDMS," in *Dekker Encyclopedia of Nanoscience and Nanotechnology*. Boca Raton, FL, USA: CRC Press, 2018.

[88] Y. Sun, W. M. Choi, H. Jiang, Y. Y. Huang, and J. A. Rogers, "Controlled buckling of semiconductor nanoribbons for stretchable electronics," *Nature Nanotechnol.*, vol. 1, no. 3, pp. 201–207, 2006.

[89] H. Gao, F. Xiao, C. B. Ching, and H. Duan, "Flexible all-solid-state asymmetric supercapacitors based on free-standing carbon nanotube/graphene and Mn_3O_4 nanoparticle/graphene paper electrodes," *ACS Appl. Mater. Interfaces*, vol. 4, no. 12, pp. 7020–7026, Dec. 2012, doi: 10.1021/am302280b.

[90] Y. Cheng, S. Lu, H. Zhang, C. V. Varanasi, and J. Liu, "Synergistic effects from graphene and carbon nanotubes enable flexible and robust electrodes for high-performance supercapacitors," *Nano Lett.*, vol. 12, no. 8, pp. 4206–4211, Aug. 2012, doi: 10.1021/nl301804c.

[91] J. Ding *et al.*, "Graphene—Vertically aligned carbon nanotube hybrid on PDMS as stretchable electrodes," *Nanotechnology*, vol. 28, no. 46, Nov. 2017, Art. no. 465302, doi: 10.1088/1361-6528/aa8ba9.

[92] R. Xu *et al.*, "Highly conductive, twistable and bendable polypyrrole–carbon nanotube fiber for efficient supercapacitor electrodes," *RSC Adv.*, vol. 5, no. 28, pp. 22015–22021, 2015, doi: 10.1039/c5ra01917f.

[93] J. Chen, Y. Liu, A. I. Minett, C. Lynam, J. Wang, and G. G. Wallace, "Flexible, aligned carbon nanotube/conducting polymer electrodes for a lithium-ion battery," *Chem. Mater.*, vol. 19, no. 15, pp. 3595–3597, Jul. 2007, doi: 10.1021/cm070991g.

[94] T. Yamada *et al.*, "A stretchable carbon nanotube strain sensor for human-motion detection," *Nature Nanotechnol.*, vol. 6, no. 5, p. 296, 2011.

[95] D. J. Lipomi *et al.*, "Skin-like pressure and strain sensors based on transparent elastic films of carbon nanotubes," *Nature Nanotechnol.*, vol. 6, no. 12, pp. 788–792, 2011.

[96] E. Roh, B. U. Hwang, D. Kim, B. Y. Kim, and N. E. Lee, "Stretchable, transparent, ultrasensitive, and patchable strain sensor for human-machine interfaces comprising a nanohybrid of carbon nanotubes and conductive elastomers," *ACS Nano*, vol. 9, no. 6, pp. 6252–6261, 2015, doi: 10.1021/acsnano.5b01613.

[97] H. Park *et al.*, "A skin-integrated transparent and stretchable strain sensor with interactive color-changing electrochromic displays," *Nanoscale*, vol. 9, no. 22, pp. 7631–7640, 2017.

[98] C. Zhang *et al.*, "Rational design of a flexible CNTs@PDMS film patterned by bio-inspired templates as a strain sensor and supercapacitor," *Small*, vol. 15, no. 18, May 2019, Art. no. 1805493, doi: 10.1002/smll.201805493.

[99] Y. Cui, "Electronic materials, devices, and signals in electrochemical sensors," *IEEE Trans. Electron Devices*, vol. 64, no. 6, pp. 2467–2477, Jun. 2017, doi: 10.1109/TED.2017.2691045.

[100] C. Chen *et al.*, "Recent advances in electrochemical glucose biosensors: A review," *RSC Adv.*, vol. 3, no. 14, pp. 4473–4491, 2013, doi: 10.1039/c2ra22351a.

[101] A. Walcarius, S. D. Minteer, J. Wang, Y. Lin, and A. Merkoçi, "Nanomaterials for bio-functionalized electrodes: Recent trends," *J. Mater. Chem. B*, vol. 1, no. 38, pp. 4878–4908, 2013, doi: 10.1039/c3tb20881h.

[102] K. K. Yeung, T. Huang, Y. Hua, K. Zhang, M. M. F. Yuen, and Z. Gao, "Recent advances in electrochemical sensors for wearable sweat monitoring: A review," *IEEE Sensors J.*, vol. 21, no. 13, pp. 14522–14539, Jul. 2021, doi: 10.1109/JSEN.2021.3074311.

[103] L. Chen, H. Xie, and W. Yu, "Functionalization methods of carbon nanotubes and its applications," in *Carbon Nanotubes Applications on Electron Devices*, vol. 41, no. 2. 2011, pp. 215–222.

[104] C. Hu, Z. Chen, A. Shen, X. Shen, J. Li, and S. Hu, "Water-soluble single-walled carbon nanotubes via noncovalent functionalization by a rigid, planar and conjugated diazo dye," *Carbon*, vol. 44, no. 3, pp. 428–434, Mar. 2006, doi: 10.1016/j.carbon.2005.09.003.

[105] Y. Zhou, Y. Fang, and R. Ramasamy, "Non-covalent functionalization of carbon nanotubes for electrochemical biosensor development," *Sensors*, vol. 19, no. 2, p. 392, Jan. 2019, doi: 10.3390/s19020392.

[106] C. A. Dyke and J. M. Tour, "Covalent functionalization of single-walled carbon nanotubes for materials applications," *J. Phys. Chem. A*, vol. 108, no. 51, pp. 11151–11159, 2004.

[107] K. A. Williams *et al.*, "Carbon nanotubes with DNA recognition," *Nature*, vol. 420, no. 6917, p. 761, 2002.

[108] A. Imani, G. Farzi, and A. Ltaief, "Facile synthesis and characterization of polypyrrole-multiwalled carbon nanotubes by *in situ* oxidative polymerization," *Int. Nano Lett.*, vol. 3, no. 1, p. 1, Dec. 2013, doi: 10.1186/2228-5326-3-52.

[109] S. A. Zaidi and J. H. Shin, "Recent developments in nanostructure based electrochemical glucose sensors," *Talanta*, vol. 149, pp. 30–42, Mar. 2016, doi: 10.1016/j.talanta.2015.11.033.

[110] H. H. Nguyen, S. H. Lee, U. J. Lee, C. D. Fermin, and M. Kim, "Immobilized enzymes in biosensor applications," *Materials*, vol. 12, no. 1, pp. 1–34, 2019, doi: 10.3390/ma12010121.

[111] B. Singh, V. Bhatia, and V. K. Jain, "Electrostatically functionalized multi-walled carbon nanotubes based flexible and non-enzymatic biosensor for glucose detection," *Sensors Transducers*, vol. 146, no. 11, pp. 69–77, 2012.

[112] V. Bhatia, V. Gaur, and V. K. Jain, "Deposition and functionalization of thin films of carbon nanotubes using corona based electrostatic charge technique and their applications for gas detection," in *Proc. 2nd Int. Workshop Electron Devices Semiconductor Technol. (IEDST)*, Jun. 2009, pp. 443–453, doi: 10.1109/EDST.2009.5166127.

[113] M. L. P. Tan, G. Lentaris, and G. A. Amaratunga, "Device and circuit-level performance of carbon nanotube field-effect transistor with benchmarking against a nano-MOSFET," *Nanosc. Res. Lett.*, vol. 7, no. 1, pp. 1–10, Dec. 2012, doi: 10.1186/1556-276X-7-467.

[114] S. Y. Oh *et al.*, "Skin-attachable, stretchable electrochemical sweat sensor for glucose and pH detection," *ACS Appl. Mater. Interfaces*, vol. 10, no. 16, pp. 13729–13740, Apr. 2018, doi: 10.1021/acsami.8b03342.

[115] A. C. Power, B. Gorey, S. Chandra, and J. Chapman, "Carbon nanomaterials and their application to electrochemical sensors: A review," *Nanotechnol. Rev.*, vol. 7, no. 1, pp. 19–41, Feb. 2018, doi: 10.1515/ntrev-2017-0160.

[116] H. S. Kim, K. U. Jang, and T. W. Kim, "NO_x gas detection characteristics in FET-type multi-walled carbon nanotube-based gas sensors for various electrode spacings," *J. Korean Phys. Soc.*, vol. 68, no. 6, pp. 797–802, Mar. 2016, doi: 10.3938/jkps.68.797.

[117] S. Bai *et al.*, "Healable, transparent, room-temperature electronic sensors based on carbon nanotube network-coated polyelectrolyte multilayers," *Small*, vol. 11, no. 43, pp. 5807–5813, Nov. 2015, doi: 10.1002/smll.201502169.

[118] J. Janata, "Chemical sensors," *Anal. Chem.*, vol. 64, no. 12, pp. 196–219, 1992.

[119] M. Li, H. Gou, I. Al-Ogaidi, and N. Wu, "Nanostructured sensors for detection of heavy metals: A review," *ACS Sustain. Chem. Eng.*, vol. 1, no. 7, pp. 713–723, 2013.

[120] S. Zhan, Y. Wu, L. Wang, X. Zhan, and P. Zhou, "A mini-review on functional nucleic acids-based heavy metal ion detection," *Biosensors Bioelectron.*, vol. 86, pp. 353–368, Dec. 2016.

[121] M. B. Gumpu, S. Sethuraman, U. M. Krishnan, and J. B. B. Rayappan, "A review on detection of heavy metal ions in water—An electrochemical approach," *Sens. Actuators B, Chem.*, vol. 213, pp. 515–533, Jul. 2015.

[122] B. Bansod, T. Kumar, R. Thakur, S. Rana, and I. Singh, "A review on various electrochemical techniques for heavy metal ions detection with different sensing platforms," *Biosensors Bioelectron.*, vol. 94, pp. 443–455, Aug. 2017.

[123] A. Paul, B. Bhattacharya, and T. K. Bhattacharyya, "Selective detection of Hg(II) over Cd(II) and Pb(II) ions by DNA functionalized CNT," *IEEE Sensors J.*, vol. 15, no. 5, pp. 2774–2779, May 2015, doi: 10.1109/JSEN.2014.2382129.

[124] C.-H. Lien, K.-H. Chang, C.-C. Hu, and D. S.-H. Wang, "Green electrode for Pb^{2+} sensing based on the Nafion-graphene/CNT composite," in *Proc. IEEE Sensors*, Oct. 2012, pp. 12–14, doi: 10.1109/ICSENS.2012.6411548.

[125] A. A. Chapin, P. R. Rajasekaran, J. Herberholz, W. E. Bentley, and R. Ghodssi, "Dynamic *in vitro* biosensing with flexible microporous multimodal cell-interfacial sensors," in *Proc. Transducers Eurosensors XXXIII*, Jun. 2019, pp. 944–947.

[126] J. Jeong, S. Kim, J. Kim, and K. Chun, "Implantable CNT-based sensor for chondroitin sulfate proteoglycans detection of glial scar after spinal cord injury," in *Proc. 8th Annu. IEEE Int. Conf. Nano/Micro Eng. Mol. Syst. (IEEE NEMS)*, Apr. 2013, pp. 1190–1193, doi: 10.1109/NEMS.2013.6559932.

[127] Q. Lu *et al.*, "Flexible paper-based Ni-MOF composite/AuNPs/CNTs film electrode for HIV DNA detection," *Biosensors Bioelectron.*, vol. 184, Jul. 2021, Art. no. 113229, doi: 10.1016/j.bios.2021.113229.

[128] H.-R. Lim *et al.*, "All-in-one, wireless, fully flexible sodium sensor system with integrated Au/CNT/Au nanocomposites," *Sens. Actuators B, Chem.*, vol. 331, Mar. 2021, Art. no. 129416, doi: 10.1016/j.snb.2020.129416.

[129] Kenry, J. C. Yeo, and C. T. Lim, "Emerging flexible and wearable physical sensing platforms for healthcare and biomedical applications," *Microsyst. Nanoeng.*, vol. 2, no. 1, p. 16043, 2016, doi: 10.1038/micronano.2016.43.

[130] Z. Lou *et al.*, "Ultrasensitive and ultraflexible e-skins with dual functionalities for wearable electronics," *Nano Energy*, vol. 38, pp. 28–35, Aug. 2017, doi: 10.1016/j.nanoen.2017.05.024.

[131] X. Lü *et al.*, "Sensitivity-compensated micro-pressure flexible sensor for aerospace vehicle," *Sensors*, vol. 19, no. 1, p. 72, Dec. 2018.

[132] S. Jung *et al.*, "Reverse-micelle-induced porous pressure-sensitive rubber for wearable human–machine interfaces," *Adv. Mater.*, vol. 26, no. 28, pp. 4825–4830, May 2014.

[133] C. Yeom, K. Chen, D. Kiriya, Z. Yu, G. Cho, and A. Javey, "Large-area compliant tactile sensors using printed carbon nanotube active-matrix backplanes," *Adv. Mater.*, vol. 27, no. 9, pp. 1561–1566, 2015.

[134] S. Stassi, V. Cauda, G. Canavese, and C. F. Pirri, "Flexible tactile sensing based on piezoresistive composites: A review," *Sensors*, vol. 14, no. 3, pp. 5296–5332, 2014.

[135] Y. Zhang *et al.*, "Polymer-embedded carbon nanotube ribbons for stretchable conductors," *Adv. Mater.*, vol. 22, no. 28, pp. 3027–3031, Jul. 2010, doi: 10.1002/adma.200904426.

[136] N. Ferrer-Anglada, V. Gomis, Z. El-Hachemi, U. D. Weglikovska, M. Kaempgen, and S. Roth, "Carbon nanotube based composites for electronic applications: CNT-conducting polymers, CNT-Cu," *Phys. Status Solidi A, Appl. Mater. Sci.*, vol. 203, no. 6, pp. 1082–1087, May 2006, doi: 10.1002/pssa.200566188.

[137] Z.-H. Jin, Y.-L. Liu, S.-L. Cai, J.-Q. Xu, W.-H. Huang, and J.-J. Chen, "Conductive polymer-coated carbon nanotubes to construct stretchable and transparent electrochemical sensors," *Anal. Chem.*, vol. 89, no. 3, pp. 2032–2038, 2017.

[138] T. Kim, D. Kim, Y. Joo, J. Park, J. Yoon, and Y. Hong, "Crack propagation design in transparent polymeric conductive films via carbon nanotube fiber-reinforcement and its application for highly sensitive and mechanically durable strain sensors," *Smart Mater. Struct.*, vol. 28, no. 2, 2018, Art. no. 025008.

[139] Z. Deng, Y. Guo, X. Zhao, P. X. Ma, and B. Guo, "Multifunctional stimuli-responsive hydrogels with self-healing, high conductivity, and rapid recovery through host–guest interactions," *Chem. Mater.*, vol. 30, no. 5, pp. 1729–1742, Mar. 2018, doi: 10.1021/acs.chemmater.8b00008.

[140] S. W. Park, P. S. Das, and J. Y. Park, "Development of wearable and flexible insole type capacitive pressure sensor for continuous gait signal analysis," *Organic Electron.*, vol. 53, pp. 213–220, Feb. 2018, doi: 10.1016/j.orgel.2017.11.033.

[141] F. A. G. da Silva, C. M. S. de Araújo, J. J. Alcaraz-Espinoza, and H. P. de Oliveira, "Toward flexible and antibacterial piezoresistive porous devices for wound dressing and motion detectors," *J. Polym. Sci. B, Polym. Phys.*, vol. 56, no. 14, pp. 1063–1072, Jul. 2018, doi: 10.1002/polb.24626.

[142] S. Y. Hong *et al.*, "Polyurethane foam coated with a multi-walled carbon nanotube/polyaniline nanocomposite for a skin-like stretchable array of multi-functional sensors," *NPG Asia Mater.*, vol. 9, no. 11, pp. 1–10, 2017, doi: 10.1038/am.2017.194.

[143] F. Ye, M. Li, D. Ke, L. Wang, and Y. Lu, "Ultrafast self-healing and injectable conductive hydrogel for strain and pressure sensors," *Adv. Mater. Technol.*, vol. 4, no. 9, Sep. 2019, Art. no. 1900346.

[144] M. Md Hossain and P. Bradford, "Industrially knittable CNT/cotton sheath-core yarns for smart textiles," *Proc. SPIE*, vol. 11378, May 2020, Art. no. 1137809, doi: 10.1117/12.2557579.

[145] L. Zhang *et al.*, "A self-protective, reproducible textile sensor with high performance towards human–machine interactions," *J. Mater. Chem. A*, vol. 7, no. 46, pp. 26631–26640, Nov. 2019, doi: 10.1039/c9ta10744d.

[146] L. Li *et al.*, "Design of a wearable and shape-memory fibriform sensor for the detection of multimodal deformation," *Nanoscale*, vol. 10, no. 1, pp. 118–123, 2018.

[147] J. Zhao, Y. Fu, Y. Xiao, Y. Dong, X. Wang, and L. Lin, "A naturally integrated smart textile for wearable electronics applications," *Adv. Mater. Technol.*, vol. 5, no. 1, pp. 1–6, 2020, doi: 10.1002/admt.201900781.

[148] Z. Ma, W. Wang, and D. Yu, "Highly sensitive and flexible pressure sensor prepared by simple printing used for micro motion detection," *Adv. Mater. Interfaces*, vol. 7, no. 2, Jan. 2020, Art. no. 1901704.

[149] G. Cai *et al.*, "Highly stretchable sheath–core yarns for multifunctional wearable electronics," *ACS Appl. Mater. Interfaces*, vol. 12, no. 26, pp. 29717–29727, Jun. 2020, doi: 10.1021/acsami.0c08840.

[150] Z. Pan *et al.*, "All-in-one stretchable coaxial-fiber strain sensor integrated with high-performing supercapacitor," *Energy Storage Mater.*, vol. 25, pp. 124–130, Mar. 2020, doi: 10.1016/j.ensm.2019.10.023.

[151] D. Hui, Y. Wu, X. Li, Y. Xiao, and M. Zhang, "Flexible pressure sensor array with tunable measurement range and high sensitivity," in *Proc. IEEE 14th Int. Conf. Nano/Micro Eng. Mol. Syst. (NEMS)*, Apr. 2019, pp. 196–200, doi: 10.1109/NEMS.2019.8915651.

[152] T. Tigerprints and C. Katsarelis. (2017). *Understanding the Impact of Strain Induced Mechanical Damage on the Electrical Performance of Metallic Thin Films*. [Online]. Available: https://tigerprints.clemson.edu/all_theses

[153] V. K. A. Devi, R. Shyam, A. Palaniappan, A. K. Jaiswal, T.-H. Oh, and A. J. Nathanael, "Self-healing hydrogels: Preparation, mechanism and advancement in biomedical applications," *Polymers*, vol. 13, no. 21, p. 3782, Oct. 2021, doi: 10.3390/polym13213782.

[154] S. Kumar *et al.*, "Review—Recent advances in the development of carbon nanotubes based flexible sensors," *J. Electrochem. Soc.*, vol. 167, no. 4, Feb. 2020, Art. no. 047506, doi: 10.1149/1945-7111/ab7331.

[155] L. Ma and W. Lu, "Carbon nanotube film based flexible bi-directional strain sensor for large deformation," *Mater. Lett.*, vol. 260, Feb. 2020, Art. no. 126959, doi: 10.1016/j.matlet.2019.126959.

[156] Z. L. Huang *et al.*, "Pyramid microstructure with single walled carbon nanotubes for flexible and transparent micro-pressure sensor with ultra-high sensitivity," *Sens. Actuators A, Phys.*, vol. 266, pp. 345–351, Oct. 2017, doi: 10.1016/j.sna.2017.09.054.

[157] M. Xu, Y. Gao, G. Yu, C. Lu, J. Tan, and F. Xuan, "Flexible pressure sensor using carbon nanotube-wrapped polydimethylsiloxane microspheres for tactile sensing," *Sens. Actuators A, Phys.*, vol. 284, pp. 260–265, Dec. 2018, doi: 10.1016/j.sna.2018.10.040.

[158] Q. Zhou, T. Chen, S. Cao, X. Xia, Y. Bi, and X. Xiao, "A novel flexible piezoresistive pressure sensor based on PVDF/PVA-CNTs electrospun composite film," *Appl. Phys. A, Solids Surf.*, vol. 127, no. 9, p. 667, Sep. 2021, doi: 10.1007/s00339-021-04797-y.

[159] Z. Qiao, A. Wei, K. Wang, N. Luo, and Z. Liu, "Study of flexible piezoresistive sensors based on the hierarchical porous structure CNT/PDMS composite materials," *J. Alloys Compounds*, vol. 917, Oct. 2022, Art. no. 165503, doi: 10.1016/j.jallcom.2022.165503.

[160] C. E. Banks, T. J. Davies, G. G. Wildgoose, and R. G. Compton, "Electrocatalysis at graphite and carbon nanotube modified electrodes: Edge-plane sites and tube ends are the reactive sites," *ChemInform*, vol. 36, no. 18, pp. 829–841, May 2005, doi: 10.1002/chin.200518203.

[161] P. Wan *et al.*, "Flexible transparent films based on nanocomposite networks of polyaniline and carbon nanotubes for high-performance gas sensing," *Small*, vol. 11, no. 40, pp. 5409–5415, Oct. 2015, doi: 10.1002/smll.201501772.

[162] S. Kim *et al.*, "Wearable, ultrawide-range, and bending-insensitive pressure sensor based on carbon nanotube network-coated porous elastomer sponges for human interface and healthcare devices," *ACS Appl. Mater. Interfaces*, vol. 11, no. 26, pp. 23639–23648, Jul. 2019, doi: 10.1021/acsami.9b07636.

[163] W.-Y. Ko, L.-T. Huang, and K.-J. Lin, "Green technique solvent-free fabrication of silver nanoparticle–carbon nanotube flexible films for wearable sensors," *Sens. Actuators A, Phys.*, vol. 317, Jan. 2021, Art. no. 112437, doi: 10.1016/j.sna.2020.112437.

[164] X. Xu *et al.*, "Copper nanowire-based aerogel with tunable pore structure and its application as flexible pressure sensor," *ACS Appl. Mater. Interfaces*, vol. 9, no. 16, pp. 14273–14280, Apr. 2017, doi: 10.1021/acsami.7b02087.

[165] H. R. Kou *et al.*, "Wireless flexible pressure sensor based on micro-patterned graphene/PDMS composite," *Sens. Actuators A, Phys.*, vol. 277, pp. 150–156, Jul. 2018, doi: 10.1016/j.sna.2018.05.015.

[166] Z. Yu, G. Cai, P. Tong, and D. Tang, "Saw-toothed microstructure-based flexible pressure sensor as the signal readout for point-of-care immunoassay," *ACS Sensors*, vol. 4, no. 9, pp. 2272–2276, Sep. 2019, doi: 10.1021/acssensors.9b01168.

[167] L. Cai and C. Wang, "Carbon nanotube flexible and stretchable electronics," *Nanosc. Res. Lett.*, vol. 10, no. 1, p. 1013, Dec. 2015, doi: 10.1186/s11671-015-1013-1.

[168] Y. Shu *et al.*, "Stretchable electrochemical biosensing platform based on Ni-MOF composite/Au nanoparticle-coated carbon nanotubes for real-time monitoring of dopamine released from living cells," *ACS Appl. Mater. Interfaces*, vol. 12, no. 44, pp. 49480–49488, Nov. 2020, doi: 10.1021/acsami.0c16060.

[169] V. Archana, Y. Xia, R. Fang, and G. G. Kumar, "Hierarchical CuO/NiO-carbon nanocomposite derived from metal organic framework on cello tape for the flexible and high performance nonenzymatic electrochemical glucose sensors," *ACS Sustain. Chem. Eng.*, vol. 7, no. 7, pp. 6707–6719, Apr. 2019, doi: 10.1021/acssuschemeng.8b05980.

[170] E. Erçarıkcı, Z. Aksu, E. Topçu, and K. D. Kıranşan, "ZnS Nanoparticles-decorated composite graphene paper: A novel flexible electrochemical sensor for detection of dopamine," *Electroanalysis*, vol. 34, no. 1, pp. 91–102, Jan. 2022, doi: 10.1002/elan.202100496.

[171] C. Zhu, Y. Xu, Q. Chen, H. Zhao, B. Gao, and T. Zhang, "A flexible electrochemical biosensor based on functionalized poly(3,4-ethylenedioxythiophene) film to detect lactate in sweat of the human body," *J. Colloid Interface Sci.*, vol. 617, pp. 454–462, Jul. 2022, doi: 10.1016/j.jcis.2022.03.029.

[172] S. M. Mugo and J. Alberkant, "Flexible molecularly imprinted electrochemical sensor for cortisol monitoring in sweat," *Anal. Bioanal. Chem.*, vol. 412, no. 8, pp. 1825–1833, Mar. 2020, doi: 10.1007/s00216-020-02430-0.

[173] M. Li, X. Liu, X. Zhao, F. Yang, X. Wang, and Y. Li, "Metallic catalysts for structure-controlled growth of single-walled carbon nanotubes," in *Single-Walled Carbon Nanotubes*. 2019, pp. 25–67.

[174] R. Vidu, M. Rahman, M. Mahmoudi, M. Enachescu, T. D. Poteca, and I. Opris, "Nanostructures: A platform for brain repair and augmentation," *Frontiers Syst. Neurosci.*, vol. 8, p. 91, Jun. 2014.

[175] A. H. Pourasl *et al.*, "Analytical modeling of glucose biosensors based on carbon nanotubes," *Nanosc. Res. Lett.*, vol. 9, no. 1, pp. 1–7, Dec. 2014.

[176] X. Xuan and J. Y. Park, "Miniaturized flexible sensor with reduced graphene oxide/carbon nano tube modified bismuth working electrode for heavy metal detection," in *Proc. IEEE 30th Int. Conf. Micro Electro Mech. Syst. (MEMS)*, Jan. 2017, pp. 636–639, doi: 10.1109/MEMSYS.2017.7863488.

[177] X. Zhang *et al.*, "Continuous graphene and carbon nanotube based high flexible and transparent pressure sensor arrays," *Nanotechnology*, vol. 26, no. 11, Mar. 2015, Art. no. 115501, doi: 10.1088/0957-4484/26/11/115501.

[178] K. Suzuki *et al.*, "Rapid-response, widely stretchable sensor of aligned MWCNT/elastomer composites for human motion detection," *ACS Sensors*, vol. 1, no. 6, pp. 817–825, Jun. 2016, doi: 10.1021/acssensors.6b00145.

[179] P. Sahatiya and S. Badhulika, "Eraser-based eco-friendly fabrication of a skin-like large-area matrix of flexible carbon nanotube strain and pressure sensors," *Nanotechnology*, vol. 28, no. 9, Jan. 2017, Art. no. 095501, doi: 10.1088/1361-6528/aa5845.

[180] W. Huang *et al.*, "Flexible and lightweight pressure sensor based on carbon nanotube/thermoplastic polyurethane-aligned conductive foam with superior compressibility and stability," *ACS Appl. Mater. Interfaces*, vol. 9, no. 48, pp. 42266–42277, Dec. 2017, doi: 10.1021/acsami.7b16975.

[181] S. Chun, W. Son, and C. Choi, "Flexible pressure sensors using highly-oriented and free-standing carbon nanotube sheets," *Carbon*, vol. 139, pp. 586–592, Nov. 2018, doi: 10.1016/j.carbon.2018.07.005.

[182] S. M. Doshi and E. T. Thostenson, "Thin and flexible carbon nanotube-based pressure sensors with ultrawide sensing range," *ACS Sensors*, vol. 3, no. 7, pp. 1276–1282, Jul. 2018, doi: 10.1021/acssensors.8b00378.

[183] L. Nela, J. Tang, Q. Cao, G. Tulevski, and S.-J. Han, "Large-area high-performance flexible pressure sensor with carbon nanotube active matrix for electronic skin," *Nano Lett.*, vol. 18, no. 3, pp. 2054–2059, Mar. 2018, doi: 10.1021/acs.nanolett.8b00063.

[184] Y. He *et al.*, "Highly stable and flexible pressure sensors with modified multi-walled carbon nanotube/polymer composites for human monitoring," *Sensors*, vol. 18, no. 5, p. 1338, Apr. 2018, doi: 10.3390/s18051338.

[185] Y. Gao, M. Xu, G. Yu, J. Tan, and F. Xuan, "Extrusion printing of carbon nanotube-coated elastomer fiber with microstructures for flexible pressure sensors," *Sens. Actuators A, Phys.*, vol. 299, Nov. 2019, Art. no. 111625, doi: 10.1016/j.sna.2019.111625.

[186] X. Sun *et al.*, "A sensitive piezoresistive tactile sensor combining two microstructures," *Nanomaterials*, vol. 9, no. 5, p. 779, 2019, doi: 10.3390/nano9050779.

[187] R. Zhang, C. Ying, H. Gao, Q. Liu, X. Fu, and S. Hu, "Highly flexible strain sensors based on polydimethylsiloxane/carbon nanotubes (CNTs) prepared by a swelling/permeating method and enhanced sensitivity by CNTs surface modification," *Compos. Sci. Technol.*, vol. 171, pp. 218–225, Feb. 2019, doi: 10.1016/j.compscitech.2018.11.034.

[188] Y. Jeong, J. Park, J. Lee, K. Kim, and I. Park, "Ultrathin, biocompatible, and flexible pressure sensor with a wide pressure range and its biomedical application," *ACS Sensors*, vol. 5, no. 2, pp. 481–489, Feb. 2020, doi: 10.1021/acssensors.9b02260.

[189] Z. Tang, S. Jia, C. Zhou, and B. Li, "3D printing of highly sensitive and large-measurement-range flexible pressure sensors with a positive piezoresistive effect," *ACS Appl. Mater. Interfaces*, vol. 12, no. 25, pp. 28669–28680, Jun. 2020, doi: 10.1021/acsami.0c06977.

[190] H. Zhong *et al.*, "Large-area flexible MWCNT/PDMS pressure sensor for ergonomic design with aid of deep learning," *Nanotechnology*, vol. 33, no. 34, May 2022, Art. no. 345502, doi: 10.1088/1361-6528/ac66ec.

[191] J. Zhu *et al.*, "Flexible pressure sensor with a wide pressure measurement range and an agile response based on multiscale carbon fibers/carbon nanotubes composite," *Microelectron. Eng.*, vol. 257, Mar. 2022, Art. no. 111750, doi: 10.1016/j.mee.2022.111750.

[192] C. Tasaltin and F. Basarir, "Preparation of flexible VOC sensor based on carbon nanotubes and gold nanoparticles," *Sens. Actuators B, Chem.*, vol. 194, pp. 173–179, Apr. 2014, doi: 10.1016/j.snb.2013.12.063.

[193] M. Asad, M. H. Sheikhi, M. Pourfath, and M. Moradi, "High sensitive and selective flexible H_2S gas sensors based on Cu nanoparticle decorated SWCNTs," *Sens. Actuators B, Chem.*, vol. 210, pp. 1–8, Apr. 2015, doi: 10.1016/j.snb.2014.12.086.

[194] L. Xue, W. Wang, Y. Guo, G. Liu, and P. Wan, "Flexible polyaniline/carbon nanotube nanocomposite film-based electronic gas sensors," *Sens. Actuators B, Chem.*, vol. 244, pp. 47–53, Jun. 2017, doi: 10.1016/j.snb.2016.12.064.

[195] T. C. Gokoglan *et al.*, "A novel approach for the fabrication of a flexible glucose biosensor: The combination of vertically aligned CNTs and a conjugated polymer," *Food Chem.*, vol. 220, pp. 299–305, Apr. 2017, doi: 10.1016/j.foodchem.2016.10.023.

[196] C. Chen *et al.*, "An efficient flexible electrochemical glucose sensor based on carbon nanotubes/carbonized silk fabrics decorated with Pt microspheres," *Sens. Actuators B, Chem.*, vol. 256, pp. 63–70, Mar. 2018, doi: 10.1016/j.snb.2017.10.067.

[197] S. Joshi, V. D. Bhatt, H. Wu, M. Becherer, and P. Lugli, "Flexible lactate and glucose sensors using electrolyte-gated carbon nanotube field effect transistor for non-invasive real-time monitoring," *IEEE Sensors J.*, vol. 17, no. 14, pp. 4315–4321, Jul. 2017, doi: 10.1109/JSEN.2017.2707521.

[198] H. Jiang and E.-C. Lee, "Highly selective, reusable electrochemical impedimetric DNA sensors based on carbon nanotube/polymer composite electrode without surface modification," *Biosensors Bioelectron.*, vol. 118, pp. 16–22, Oct. 2018, doi: 10.1016/j.bios.2018.07.037.

[199] B. Liu *et al.*, "A flexible NO_2 gas sensor based on polypyrrole/nitrogen-doped multiwall carbon nanotube operating at room temperature," *Sens. Actuators B, Chem.*, vol. 295, pp. 86–92, Sep. 2019, doi: 10.1016/j.snb.2019.05.065.

[200] P. Zhu *et al.*, "Flexible and highly sensitive humidity sensor based on cellulose nanofibers and carbon nanotube composite film," *Langmuir*, vol. 35, no. 14, pp. 4834–4842, Apr. 2019, doi: 10.1021/acs.langmuir.8b04259.

[201] P. Gulati, P. Mishra, M. Khanuja, J. Narang, and S. S. Islam, "Nanomoles detection of tumor specific biomarker DNA for colorectal cancer detection using vertically aligned multi-wall carbon nanotubes based flexible electrodes," *Process Biochem.*, vol. 90, pp. 184–192, Mar. 2020, doi: 10.1016/j.procbio.2019.11.021.

[202] C. J. Valentine, K. Takagishi, S. Umezu, R. Daly, and M. De Volder, "Paper-based electrochemical sensors using paper as a scaffold to create porous carbon nanotube electrodes," *ACS Appl. Mater. Interfaces*, vol. 12, no. 27, pp. 30680–30685, Jul. 2020, doi: 10.1021/acsami.0c04896.

[203] L. Yang, Y. Wu, F. Yang, and W. Wang, "A conductive polymer composed of a cellulose-based flexible film and carbon nanotubes," *RSC Adv.*, vol. 11, no. 33, pp. 20081–20088, Jun. 2021, doi: 10.1039/d1ra03474j.

[204] J. Li, M. Jiang, M. Su, L. Tian, W. Shi, and C. Yu, "Stretchable and transparent electrochemical sensor based on nanostructured au on carbon nanotube networks for real-time analysis of H_2O_2 release from cells," *Anal. Chem.*, vol. 93, no. 17, pp. 6723–6730, May 2021, doi: 10.1021/acs.analchem.1c00336.

[205] T. Jiang *et al.*, "A rigidity/flexibility compatible strategy to improve the stability and durability of flexible electrochemical sensor based on a polydimethylsiloxane membrane supported Prussian blue@carbon nanotube array," *Electroanalysis*, vol. 34, no. 4, pp. 655–658, Apr. 2022, doi: 10.1002/elan.202100274.

[206] S. Nasraoui *et al.*, "Electrochemical sensor for nitrite detection in water samples using flexible laser-induced graphene electrodes functionalized by CNT decorated by Au nanoparticles," *J. Electroanal. Chem.*, vol. 880, Jan. 2021, Art. no. 114893, doi: 10.1016/j.jelechem.2020.114893.

[207] T. Someya, T. Sekitani, S. Iba, Y. Kato, H. Kawaguchi, and T. Sakurai. (2004). *A Large-Area, Flexible Pressure Sensor Matrix With Organic Field-Effect Transistors for Artificial Skin Applications*. [Online]. Available: https://www.pnas.orgcgidoi10.1073pnas.0401918101

[208] Y. Joo *et al.*, "Silver nanowire-embedded PDMS with a multiscale structure for a highly sensitive and robust flexible pressure sensor," *Nanoscale*, vol. 7, no. 14, pp. 6208–6215, 2015, doi: 10.1039/C5NR00313J.

[209] B.-Y. Lee, J. Kim, H. Kim, C. Kim, and S.-D. Lee, "Low-cost flexible pressure sensor based on dielectric elastomer film with micro-pores," *Sens. Actuators A, Phys.*, vol. 240, pp. 103–109, Apr. 2016.

[210] C. Lou *et al.*, "A graphene-based flexible pressure sensor with applications to plantar pressure measurement and gait analysis," *Materials*, vol. 10, no. 9, p. 1068, Sep. 2017.

[211] X. Shuai *et al.*, "Highly sensitive flexible pressure sensor based on silver nanowires-embedded polydimethylsiloxane electrode with microarray structure," *ACS Appl. Mater. Interfaces*, vol. 9, no. 31, pp. 26314–26324, Aug. 2017, doi: 10.1021/acsami.7b05753.

[212] A. Al-Saygh, D. Ponnamma, M. AlMaadeed, P. Vijayan P, A. Karim, and M. Hassan, "Flexible pressure sensor based on PVDF nanocomposites containing reduced graphene oxide-titania hybrid nanolayers," *Polymers*, vol. 9, no. 12, p. 33, Jan. 2017.

[213] G. Wang *et al.*, "Flexible pressure sensor based on PVDF nanofiber," *Sens. Actuators A, Phys.*, vol. 280, pp. 319–325, Sep. 2018, doi: 10.1016/j.sna.2018.07.057.

[214] J. Shi *et al.*, "Multiscale hierarchical design of a flexible piezoresistive pressure sensor with high sensitivity and wide linearity range," *Small*, vol. 14, no. 27, Jul. 2018, Art. no. 1800819, doi: 10.1002/smll.201800819.

[215] Y. Ai *et al.*, "An ultrasensitive flexible pressure sensor for multimodal wearable electronic skins based on large-scale polystyrene ball@reduced graphene-oxide core–shell nanoparticles," *J. Mater. Chem. C*, vol. 6, no. 20, pp. 5514–5520, 2018, doi: 10.1039/C8TC01153B.

[216] T. Li *et al.*, "A flexible pressure sensor based on an MXene–textile network structure," *J. Mater. Chem. C*, vol. 7, no. 4, pp. 1022–1027, Jan. 2019, doi: 10.1039/C8TC04893B.

[217] H. Guan, J. Meng, Z. Cheng, and X. Wang, "Processing natural wood into a high-performance flexible pressure sensor," *ACS Appl. Mater. Interfaces*, vol. 12, no. 41, pp. 46357–46365, Oct. 2020, doi: 10.1021/acsami.0c12561.

[218] M. Li, J. Liang, X. Wang, and M. Zhang, "Ultra-sensitive flexible pressure sensor based on microstructured electrode," *Sensors*, vol. 20, no. 2, p. 371, Jan. 2020.

[219] M. Fu, J. Zhang, Y. Jin, Y. Zhao, S. Huang, and C. F. Guo, "A highly sensitive, reliable, and high-temperature-resistant flexible pressure sensor based on ceramic nanofibers," *Adv. Sci.*, vol. 7, no. 17, Sep. 2020, Art. no. 2000258, doi: 10.1002/advs.202000258.

[220] Y. Wang, W. Zhu, Y. Yu, P. Zhu, Q. Song, and Y. Deng, "High-sensitivity flexible pressure sensor with low working voltage based on sphenoid microstructure," *IEEE Sensors J.*, vol. 20, no. 13, pp. 7354–7361, Jul. 2020, doi: 10.1109/JSEN.2020.2978655.

[221] M. Zhong *et al.*, "Wide linear range and highly sensitive flexible pressure sensor based on multistage sensing process for health monitoring and human-machine interfaces," *Chem. Eng. J.*, vol. 412, May 2021, Art. no. 128649, doi: 10.1016/j.cej.2021.128649.

[222] Z. Duan *et al.*, "A do-it-yourself approach to achieving a flexible pressure sensor using daily use materials," *J. Mater. Chem. C*, vol. 9, no. 39, pp. 13659–13667, Oct. 2021, doi: 10.1039/D1TC03102C.

[223] B. Xue, H. Xie, J. Zhao, J. Zheng, and C. Xu, "Flexible piezoresistive pressure sensor based on electrospun rough polyurethane nanofibers film for human motion monitoring," *Nanomaterials*, vol. 12, no. 4, p. 723, Feb. 2022, doi: 10.3390/nano12040723.

[224] M. Santhiago, M. Strauss, M. P. Pereira, A. S. Chagas, and C. C. B. Bufon, "Direct drawing method of graphite onto paper for high-performance flexible electrochemical sensors," *ACS Appl. Mater. Interfaces*, vol. 9, no. 13, pp. 11959–11966, Apr. 2017, doi: 10.1021/acsami.6b15646.

[225] T. Gan, Z. Wang, Y. Wang, X. Li, J. Sun, and Y. Liu, "Flexible graphene oxide–wrapped SnO_2 hollow spheres with high electrochemical sensing performance in simultaneous determination of 4–aminophenol and 4–chlorophenol," *Electrochim. Acta*, vol. 250, pp. 1–9, Oct. 2017, doi: 10.1016/j.electacta.2017.08.043.

[226] M. Santhiago *et al.*, "Flexible and foldable fully-printed carbon black conductive nanostructures on paper for high-performance electronic, electrochemical, and wearable devices," *ACS Appl. Mater. Interfaces*, vol. 9, no. 28, pp. 24365–24372, Jul. 2017, doi: 10.1021/acsami.7b06598.

[227] R. Zhong *et al.*, "Self-assembly of enzyme-like nanofibrous G-molecular hydrogel for printed flexible electrochemical sensors," *Adv. Mater.*, vol. 30, no. 12, Mar. 2018, Art. no. 1706887.

[228] R. Sha, N. Vishnu, and S. Badhulika, "MoS_2 based ultra-low-cost, flexible, non-enzymatic and non-invasive electrochemical sensor for highly selective detection of uric acid in human urine samples," *Sens. Actuators B, Chem.*, vol. 279, pp. 53–60, Jan. 2019, doi: 10.1016/j.snb.2018.09.106.

[229] L. Manjakkal, B. Sakthivel, N. Gopalakrishnan, and R. Dahiya, "Printed flexible electrochemical pH sensors based on CuO nanorods," *Sens. Actuators B, Chem.*, vol. 263, pp. 50–58, Jun. 2018, doi: 10.1016/j.snb.2018.02.092.

[230] M. Bariya *et al.*, "Roll-to-roll gravure printed electrochemical sensors for wearable and medical devices," *ACS Nano*, vol. 12, no. 7, pp. 6978–6987, Jul. 2018, doi: 10.1021/acsnano.8b02505.

[231] E. Aparicio-Martínez, A. Ibarra, I. A. Estrada-Moreno, V. Osuna, and R. B. Dominguez, "Flexible electrochemical sensor based on laser scribed graphene/Ag nanoparticles for non-enzymatic hydrogen peroxide detection," *Sens. Actuators B, Chem.*, vol. 301, Dec. 2019, Art. no. 127101, doi: 10.1016/j.snb.2019.127101.

[232] I. A. de Araujo Andreotti *et al.*, "Disposable and flexible electrochemical sensor made by recyclable material and low cost conductive ink," *J. Electroanal. Chem.*, vol. 840, pp. 109–116, May 2019, doi: 10.1016/j.jelechem.2019.03.059.

[233] G. Xu *et al.*, "Smartphone-based battery-free and flexible electrochemical patch for calcium and chloride ions detections in biofluids," *Sens. Actuators B, Chem.*, vol. 297, Oct. 2019, Art. no. 126743, doi: 10.1016/j.snb.2019.126743.

[234] J. Yoon *et al.*, "Flexible electrochemical glucose biosensor based on GO_x/gold/MoS_2/gold nanofilm on the polymer electrode," *Biosensors Bioelectron.*, vol. 140, Sep. 2019, Art. no. 111343, doi: 10.1016/j.bios.2019.111343.

[235] X. Hui, X. Xuan, J. Kim, and J. Y. Park, "A highly flexible and selective dopamine sensor based on Pt-Au nanoparticle-modified laser-induced graphene," *Electrochim. Acta*, vol. 328, Dec. 2019, Art. no. 135066, doi: 10.1016/j.electacta.2019.135066.

[236] R. Li *et al.*, "A flexible and physically transient electrochemical sensor for real-time wireless nitric oxide monitoring," *Nature Commun.*, vol. 11, no. 1, p. 3207, Dec. 2020, doi: 10.1038/s41467-020-17008-8.

[237] D. Ji *et al.*, "Smartphone-based square wave voltammetry system with screen-printed graphene electrodes for norepinephrine detection," *Smart Mater. Med.*, vol. 1, pp. 1–9, Jan. 2020.

[238] G. C. M. D. Oliveira, J. H. D. S. Carvalho, L. C. Brazaca, N. C. S. Vieira, and B. C. Janegitz, "Flexible platinum electrodes as electrochemical sensor and immunosensor for Parkinson's disease biomarkers," *Biosensors Bioelectron.*, vol. 152, Mar. 2020, Art. no. 112016, doi: 10.1016/j.bios.2020.112016.

[239] A. B. Patil *et al.*, "Flexible and disposable gold nanoparticles-N-doped carbon-modified electrochemical sensor for simultaneous detection of dopamine and uric acid," *Nanotechnology*, vol. 32, no. 6, Feb. 2021, Art. no. 065502, doi: 10.1088/1361-6528/abc388.

[240] F. Gao *et al.*, "All-polymer free-standing electrodes for flexible electrochemical sensors," *Sens. Actuators B, Chem.*, vol. 334, May 2021, Art. no. 129675, doi: 10.1016/j.snb.2021.129675.

[241] P. Pathak *et al.*, "Flexible copper-biopolymer nanocomposite sensors for trace level lead detection in water," *Sens. Actuators B, Chem.*, vol. 344, Oct. 2021, Art. no. 130263, doi: 10.1016/j.snb.2021.130263.

[242] J. Li and X. Bo, "Laser-enabled flexible electrochemical sensor on finger for fast food security detection," *J. Hazardous Mater.*, vol. 423, Feb. 2022, Art. no. 127014, doi: 10.1016/j.jhazmat.2021.127014.

[243] G. Zhao, X. Wang, G. Liu, and N. T. D. Thuy, "A disposable and flexible electrochemical sensor for the sensitive detection of heavy metals based on a one-step laser-induced surface modification: A new strategy for the batch fabrication of sensors," *Sens. Actuators B, Chem.*, vol. 350, Jan. 2022, Art. no. 130834.

[244] J. M. Nugent, K. S. V. Santhanam, A. Rubio, and P. M. Ajayan, "Fast electron transfer kinetics on multiwalled carbon nanotube microbundle electrodes," *Nano Lett.*, vol. 1, no. 2, pp. 87–91, Feb. 2001, doi: 10.1021/nl005521z.

[245] Y. Sun *et al.*, "Suspended CNT-based FET sensor for ultrasensitive and label-free detection of DNA hybridization," *Biosensors Bioelectron.*, vol. 137, pp. 255–262, Jul. 2019, doi: 10.1016/j.bios.2019.04.054.

[246] X. Yao, Y. Zhang, W. Jin, Y. Hu, and Y. Cui, "Carbon nanotube field-effect transistor-based chemical and biological sensors," *Sensors*, vol. 21, no. 3, pp. 1–18, Feb. 2021, doi: 10.3390/s21030995.

[247] P.-L. Ong, W. B. Euler, and I. A. Levitsky, "Hybrid solar cells based on single-walled carbon nanotubes/Si heterojunctions," *Nanotechnology*, vol. 21, no. 10, Mar. 2010, Art. no. 105203, doi: 10.1088/0957-4484/21/10/105203.

[248] S. Peng *et al.*, "Carbon nanotube chemical and mechanical sensors," in *Proc. 3rd Int. Workshop Struct. Health Monit.*, 2001, pp. 1–8.

[249] G. Valdés-Ramírez *et al.*, "Microneedle-based self-powered glucose sensor," *Electrochem. Commun.*, vol. 47, pp. 58–62, Oct. 2014, doi: 10.1016/j.elecom.2014.07.014.

[250] E. Song and J.-W. Choi, "Self-calibration of a polyaniline nanowire-based chemiresistive pH sensor," *Microelectronic Eng.*, vol. 116, pp. 26–32, Mar. 2014, doi: 10.1016/j.mee.2013.10.014.

[251] E. Song, T. H. da Costa, and J.-W. Choi, "A chemiresistive glucose sensor fabricated by inkjet printing," *Microsyst. Technol.*, vol. 23, no. 8, pp. 3505–3511, Aug. 2017, doi: 10.1007/s00542-016-3160-4.